

# Air Toxics Hot Spots Program

## Perchloroethylene Inhalation Cancer Unit Risk Factor

Technical Support Document for Cancer  
Potency Factors

Appendix B

SRP Review Draft

May 2016 [revised](#)



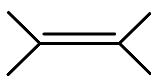
Air, Community, and Environmental Research Branch  
Office of Environmental Health Hazard Assessment  
California Environmental Protection Agency

**Page left intentionally blank**

List of Acronyms

AIC	Akaike information criterion	<del>MCL</del>	<del>Mononuclear cell leukemia</del>
AUC	Area under the concentration curve	MCMC	Markov Chain Monte Carlo method
BMD	Benchmark Dose	mg-hr/(L-d)	Milligram-hours per liter per day
BMDL	Estimation of the BMD 95% lower	mg/kg-d	Milligram per kilogram per day
BMDs	Benchmark Dose Software	µg/m <sup>3</sup>	Microgram per cubic meter
BW	Body weight	MLE	Maximum likelihood estimate
CDPH	California Department of Health Services	MOA	Mode of action
CYP450	Cytochrome P450	N-AcTCVC	N-acetyl-S-(1,2,2-trichlorovinyl)cysteine
DCA	Dichloroacetic acid	NAT	N-acetyl transferase
DEHP	Diethyl hexyl phthalate	NCI	National Cancer Institute
DNA	Deoxyribose nucleic acid	NRC	National Research Council
<del>DCVG</del>	<del>S-(1,2-dichlorovinyl)-glutathione</del>	NTP	National Toxicology Program
FMO3	Flavin-containing mono-oxygenase 3	PBPK	Physiologically-based pharmacokinetic
GLP	Good Laboratory Practice standards	PCE	Perchloroethylene
GSH	Glutathione	PHG	Public Health Goal
GST	Glutathione-S-transferase	PPARα	Peroxisome proliferator-activated receptor-α
HEC	Human equivalent concentration	ppb	Parts per billion
IARC	International Agency for Research on Cancer	ppm	Parts per million
IRIS	Integrated risk information system (US EPA)	TAC	Toxic Air Contaminant
JBRC	Japan Bioassay Research Center	TCA	Trichloroacetic acid
JISHA	Japan Industrial Safety and Health Association	TCE	Trichloroethylene
LGLL	Large granular lymphocyte leukemia	TCVC	S-(trichlorovinyl)cysteine
<del>MCL</del>	<del>Mononuclear cell leukemia</del>	TCVG	S-(1,2,2-trichlorovinyl)-glutathione
		TSD	Technical Support Document
		URF	Unit risk factor
		US EPA	U.S. Environmental Protection Agency
		VOC	Volatile organic compound

1 **PERCHLOROETHYLENE**  
2



3  
4 CAS Number: 127-18-4  
5

6 **1. INTRODUCTION**

7 The Office of Environmental Health Hazard Assessment (OEHHA) develops potency  
8 values for carcinogenic substances that are candidate Toxic Air Contaminants (TACs)  
9 (Health and Safety Code Section 39660) or are listed under the Air Toxics Hot Spots  
10 Act (Health and Safety Code Section 44321). These values are used in the Air  
11 Resources Board's (ARB's) air toxics control programs and also by other State  
12 regulatory bodies, to estimate cancer risk in humans.  
13

14 Perchloroethylene (PCE), also commonly referred to as tetrachloroethylene, was  
15 officially placed on the TAC list by the ARB in 1991. In support of that decision, the  
16 California Department of Health Services evaluated the toxicology of PCE and  
17 determined that it was a potential carcinogen in humans, besides displaying other forms  
18 of toxicity (CDHS, 1991). Shortly thereafter, OEHHA derived inhalation potency values  
19 for PCE using dose-response data from a National Toxicology Program (NTP) study of  
20 the chemical's carcinogenic effects in rodents (OEHHA, 1992; NTP, 1986). OEHHA's  
21 potency values were based upon the induction of liver tumors in male mice and  
22 incorporated a simple pharmacokinetic model to estimate internal metabolized doses.  
23

24 The present document updates the dose-response analysis for inhalation exposure to  
25 PCE to derive a cancer unit risk factor (expressed as  $(\mu\text{g}/\text{m}^3)^{-1}$ ) and a corresponding  
26 cancer slope factor (expressed in  $(\text{mg}/\text{kg}\text{-d})^{-1}$ ) using OEHHA's current Air Toxics Hot  
27 Spots program risk assessment guidelines (OEHHA, 2009), and research made  
28 available since our last PCE review in 1992. In particular, OEHHA has identified an  
29 additional well-conducted, lifetime rodent inhalation study (JISHA, 1993); also, a refined  
30 physiologically-based pharmacokinetic (PBPK) model for PCE has been published  
31 (Chiu and Ginsberg, 2011). Both of these studies were used in the update. Where  
32 appropriate, the current analysis draws upon material from previous OEHHA  
33 evaluations, as well as recent toxicological assessments published by the US  
34 Environmental Protection Agency (US EPA, 2012a) and the International Agency for  
35 Research on Cancer (IARC, 2014).  
36

37 **2. SUMMARY OF DERIVED VALUES**

38 OEHHA's revised potency values for PCE are based on the elevated incidence of  
39 several tumor types observed in male mice and rats in relation to PCE-metabolized  
40 doses calculated with a simplified adaptation of the Chiu and Ginsberg (2011) model. For  
41 dose-response calculations, OEHHA used US EPA's Benchmark Dose Software (BMDS)  
42 (US EPA, 2015) and its implementation of the multi-stage cancer model. BMDS was also

43 used to evaluate the multi-site tumor risks. After considering several issues related to  
 44 data quality and analytical uncertainty, the geometric mean of 4 dose-response values  
 45 was chosen as the best estimate of carcinogenic potency. The potency values for PCE,  
 46 in terms of external exposure, are:  
 47

Unit Risk Factor ( $\mu\text{g}/\text{m}^3$ ) <sup>-1</sup>	6.1E-06
Slope Factor ( $\text{mg}/\text{kg}\cdot\text{day}$ ) <sup>-1</sup>	2.1E-02

48  
 49 **3. MAJOR SOURCES AND USES**

50 PCE is a dense volatile liquid with an ether-like odor. It is used mainly as a chemical  
 51 intermediate, solvent, and cleaning agent. The total US demand for PCE in 2004 was  
 52 355 million pounds (Dow, 2008). In the US, 60 percent of PCE use was for chemical  
 53 production (e.g., to make hydrofluorocarbon alternatives to chlorofluorocarbons), 18  
 54 percent was used in surface preparation and cleaning, 18 percent in dry-cleaning and  
 55 textile processing, and 4 percent for miscellaneous other uses (*ibid.*). Total air  
 56 emissions of PCE in California for 2010 were estimated by ARB to be 3832 tons per  
 57 year (ARB, 2012).  
 58

59 **4. SELECTED PHYSICAL AND CHEMICAL PROPERTIES OF PCE**  
 60

Molecular weight	165.83
Boiling point	121 °C
Melting point	-19 °C
Vapor pressure	18.47 mm Hg @ 25 °C
Air concentration conversion	1 ppm = 6.78 mg/m <sup>3</sup> @ 25 °C

(HSDB, 2010)

61  
 62 **5. NATIONAL AND INTERNATIONAL HAZARD EVALUATIONS**

63 According to the National Toxicology Program (NTP) 13th Report on Carcinogens  
 64 (RoC), PCE is "reasonably anticipated to be a human carcinogen based on sufficient  
 65 evidence of carcinogenicity from studies in experimental animals" (NTP, 2014). The  
 66 RoC found that PCE exposure produced tumors in multiple tissue types of both sexes of  
 67 mice and rats. For inhalation exposure, the tumor types cited by NTP were:  
 68 mononuclear-cell leukemia in rats, tubular-cell kidney tumors in male rats and liver  
 69 tumors in mice. Additionally, NTP noted increased liver tumors in mice exposed to PCE  
 70 by ingestion.  
 71

72 IARC found that PCE is "probably carcinogenic to humans," citing limited  
 73 epidemiological findings (primarily increased bladder cancer in dry cleaning workers)  
 74 and sufficient evidence in experimental animals (IARC, 2014). For rodents, in addition to  
 75 the tumor types noted by NTP, IARC notes an increased incidence of: hemangioma and  
 76 hemangiosarcoma of the liver in mice, spleen and Harderian gland tumors in male mice,

77 brain and testicular tumors in male rats, and skin tumors in mice dermally exposed to  
78 the PCE metabolite, tetrachloroethylene oxide.

79  
80 US EPA states that PCE is “likely to be carcinogenic in humans by all routes of  
81 exposure,” based upon suggestive epidemiologic data (bladder cancer, non-Hodgkin’s  
82 lymphoma, and multiple myeloma) and conclusive evidence from carcinogenicity  
83 studies in rodents (referring to the same set of tumors as above) (US EPA, 2012b).

84  
85 PCE has been listed on California’s Proposition 65 list since 1988 as a chemical “known  
86 to the state to cause cancer.” California’s Public Health Goal for drinking water is based  
87 on PCE-induced carcinogenicity (OEHHA, 2001).

## 88 89 **6. TOXICOKINETICS**

90 PCE is readily absorbed through the lungs and gastrointestinal tract, and can also be  
91 absorbed to a lesser extent through the skin. The blood-air partition coefficients of PCE  
92 in humans and rodents are in the range of about 15 to 20 (Chiu and Ginsberg, 2011).  
93 These values indicate the ratio by which the PCE concentration in blood will be greater  
94 than its concentration in air at equilibrium. Humans breathing air containing 100 ppm  
95 PCE over 8 hours absorbed approximately 70 percent of inhaled PCE after the first  
96 hour, and 50 percent of the PCE intake at the end of the exposure period (Fernandez,  
97 *et al.*, 1976). Once in the body, PCE disperses into all tissues, concentrating  
98 preferentially in fatty tissues. For example, in rats inhaling 500 ppm PCE for 2 hours, the  
99 area under the concentration curve (AUC) after 72 hours, in milligram-minutes per  
100 milliliter of tissue, was: 1493 (fat), 33 (brain), 31 (liver), 26 (kidney), and 8.4 (blood)  
101 (Dallas, *et al.*, 1994).

102  
103 PCE has a relatively low rate of metabolism in rodents and humans and is primarily  
104 eliminated unchanged via exhalation. In rats exposed to 150 ppm PCE in drinking water  
105 for 12 hours and monitored for an additional 72 hours, approximately 88% of the body  
106 burden was eliminated unmetabolized by exhalation (Frantz and Watanabe, 1983).  
107 Ohtsuki, *et al.* (1983) monitored occupationally exposed dry-cleaning workers and  
108 estimated that at the end of an 8-hour exposure to 50 ppm, about 38% of absorbed  
109 PCE was exhaled unchanged and 2% metabolized and excreted in urine.

### 110 111 PCE Metabolites

112 The metabolism of perchloroethylene has been studied mostly in mice, rats, and  
113 humans. Detailed reviews of this literature have been published (Lash and Parker,  
114 2001; Anders *et al.*, 1988; Dekant, 1986). Briefly, rodent studies have identified the  
115 following urinary metabolites:

- 116  
117
- 118 • trichloroacetic acid (TCA)
  - 119 • N-trichloroacetyl aminoethanol
  - 120 • oxalic acid
  - 121 • N-oxalylaminoethanol
  - dichloroacetic acid (DCA)

- 122 • S-(1,2,2-trichlorovinyl)glutathione (TCVG)
- 123 • N-acetyl-S-(1,2,2-trichlorovinyl)cysteine (N-AcTCVC)

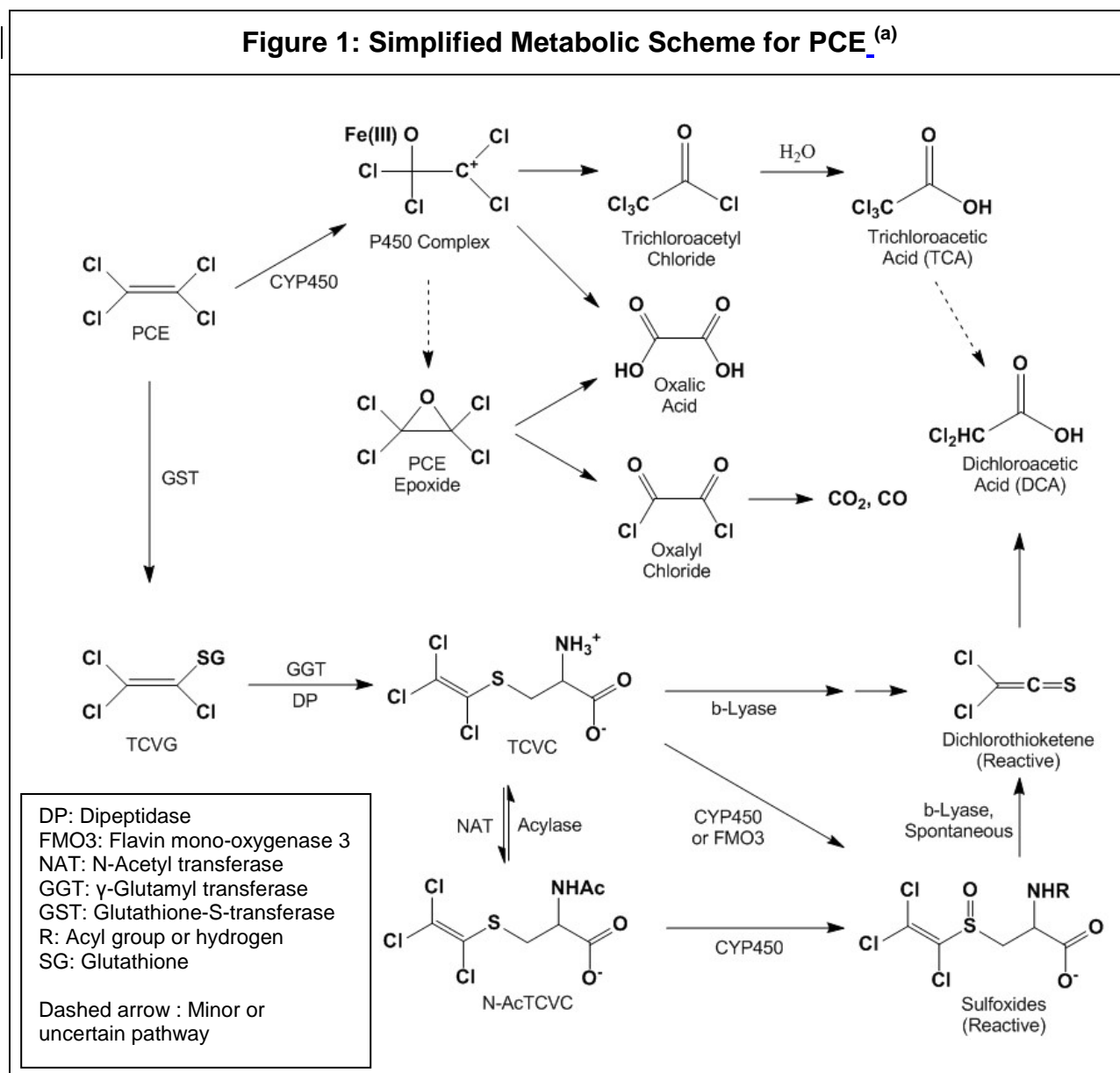
124  
125 Trichloroacetic acid and N-AcTCVC have also been observed in the urine of exposed  
126 humans. The aminoethanol derivatives, N-trichloroacetyl aminoethanol and oxalyl  
127 aminoethanol, are thought to arise from the reaction of the intermediate acyl chlorides  
128 with phosphatidyl ethanolamine present in biological membranes (Dekant, *et al.*, 1986).  
129 Carbon dioxide has also been found as an exhaled metabolite. Trichloroethanol has  
130 been detected in urine samples in some studies, but not in others, and it is unclear  
131 whether it was produced from co-exposure to trichloroethylene (in occupational  
132 exposures), or in other cases, if it was an artifact of the analytical methods employed  
133 (Lash and Parker, 2001). More recent work (e.g., Yoshioka, *et al.*, 2002) has not  
134 detected trichloroethanol and supports the conclusion that it is not a significant PCE  
135 metabolite (US EPA, 2012a).

136  
137 A simplified metabolic scheme for PCE is presented in Figure 1. Two main pathways of  
138 metabolism have been identified. The first, referred to here as the "oxidative pathway,"  
139 involves oxidation of PCE by Cytochrome P450 (CYP450) enzymes. CYP2E1 is thought  
140 to be the primary isoform involved, with additional participation of isoforms 2B1/2, and  
141 3A4. The main metabolic product of the oxidative pathway is trichloroacetic acid (TCA),  
142 formed by hydrolysis of intermediate trichloroacetyl chloride, the latter of which appears  
143 to be formed by molecular rearrangement of the substrate-CYP450 complex (Guyton, *et al.*,  
144 2014). A secondary product is the reactive tetrachloroethylene oxide (PCE epoxide),  
145 which decomposes to oxalyl chloride and then to carbon monoxide and carbon dioxide  
146 (Yoshioka, *et al.*, 2002). Oxalic acid may also form from decomposition of PCE epoxide  
147 or directly from the substrate-enzyme complex. (Guyton *et al.*, 2014).

148  
149 The second metabolic pathway for PCE (the "GST pathway") is initiated by glutathione-  
150 S-transferase (GST)-catalyzed conjugation with glutathione (GSH), forming S-  
151 (trichlorovinyl)glutathione (TCVG). This conjugate can undergo additional enzymatic  
152 transformations to reactive and potentially genotoxic intermediates. First, the tripeptide  
153 glutathione moiety of TCVG is degraded via hydrolytic cleavage of its glycine and  
154 glutamine units, producing S-(trichlorovinyl)cysteine (TCVC). TCVC may be  
155 subsequently transformed as follows:

- 156  
157 • The free amino group of TCVC may be acylated by N-acetyl transferase, forming  
158 N-acetyl-S-(trichlorovinyl)cysteine (N-AcTCVC) which passes into urine; this  
159 process may also be reversed by acylases, regenerating TCVC.
- 160 • The sulfur atom of TCVC and N-AcTCVC may be oxidized by CYP450 or flavin-  
161 containing mono-oxygenase 3 (FMO3); this process forms reactive  $\alpha,\beta$ -  
162 unsaturated sulfoxides that can bond with nucleophilic biological molecules or  
163 spontaneously decompose to dichlorothioketene, itself a reactive metabolite.

164



(a) From Guyton *et al.* (2014), US EPA (2012a), and Lash and Parker (2001).

- 165       • The carbon-sulfur bond of TCVC may be cleaved by  $\beta$ -lyase, releasing an  
 166       unstable trichlorovinyl thiol that spontaneously decomposes to  
 167       dichlorothioketene.  
 168

169       Dichloroacetic acid, believed to arise mainly by hydrolysis of dichlorothioketene, was  
 170       found in rat but not human urine. Evidence for this mechanism comes from the detection  
 171       of a covalent protein adduct N-(dichloroacetyl)-L-lysine in rat kidney cells (Birner *et al.*,  
 172       1994).

173

174 Multi-Organ Metabolism

175 The toxicokinetic behavior of PCE is somewhat complicated due to the variety of  
176 potentially genotoxic metabolites that can be produced, and because significant PCE  
177 metabolism occurs in both the liver and kidney (and possibly other organs as well). The  
178 liver is considered the main site of metabolism for the oxidative pathway. In this pathway,  
179 initial oxidation by CYP450, produces several reactive intermediates that can rearrange,  
180 hydrolyze, undergo conjugation, and otherwise decompose to more stable and soluble  
181 metabolites that can then be eliminated in the urine or by exhalation. Other tissues with  
182 appropriate CYP450 activity, e.g., lung, kidney, brain, and lymphocytes,<sup>1</sup> may also  
183 independently oxidize PCE, though to a smaller extent.

184  
185 The GST pathway involves a series of enzymatic transformations with cycling of  
186 metabolic intermediates mainly between the liver and kidney, and including some entero-  
187 hepatic processing. In this pathway, the initial glutathione conjugation step occurs  
188 primarily in the liver, forming TCVG which is then transported to the blood and bile. The  
189 kidney epithelium actively absorbs the circulating glutathione conjugate for further  
190 processing and excretion. As noted above, this involves cleavage of TCVG by gamma  
191 glutamyl transferase (GGT) and dipeptidase (DP) to form TCVC. The amino group of  
192 TCVC can then be acylated to form mercapturate N-AcTCVC in the kidney, or TCVC  
193 may recirculate back to the liver for acylation (Lash and Parker, 2001).

194  
195 In some species, such as rabbit and guinea pig, significant intrahepatic processing of  
196 glutathione conjugates may occur, with formation of TCVC from TCVG by the bile-duct  
197 epithelium, followed by reabsorption into hepatocytes and subsequent acylation.  
198 Additionally, TCVG excreted via the bile can be converted to TCVC in the intestinal  
199 lumen and undergo entero-hepatic cycling (Hinchman and Ballatori, 1994; Irving and  
200 Elfarra, 2013).

201  
202 The kidney is viewed as the main site for formation of genotoxic metabolites by  $\beta$ -lyase  
203 cleavage of TCVC since  $\beta$ -lyase activity is relatively high in this organ. Smaller amounts  
204 of  $\beta$ -lyase have been found in other organs, such as the liver, brain, and spleen  
205 (Rooseboom, *et al.*, 2002), raising the possibility that reactive dichlorothioketene may be  
206 generated and produce genetic damage in other tissues independent of its production in  
207 the kidney. Although the liver contains a form of  $\beta$ -lyase, enzymatic cleavage of TCVC  
208 does not appear to be significant in this organ. For example, in rats treated with the PCE-  
209 conjugate analogues, dichlorovinyl glutathione (DCVG) and dichlorovinyl cysteine  
210 (DCVC), significant pathology was observed in the kidney, but no tissue damage was  
211 seen in the liver (Lash and Parker, 2001).

212  
213 Oxidation of TCVC and N-AcTCVC to the reactive  $\alpha,\beta$ -unsaturated sulfoxides can occur  
214 in the liver and kidney, as well as other organs that contain flavin mono-oxygenase 3  
215 (FMO3) or CYP450 3A activity. As noted above, the sulfoxides are reactive Michael  
216 acceptors and can bond with nucleophilic sites on biological molecules. Discussing the

---

<sup>1</sup> Lymphocyte microsomes from male Wistar rats have been found to contain CYP450 2B, 2E, and 3A activity at 20, 4, and 2.4 percent of liver microsomal activity. Lymphocyte CYP450 content can also be chemically induced, resulting in 2 to 4-fold increases in activity (Hannon-Fletcher and Barnett, 2008).

217 metabolism of trichloroethylene (TCE), Irving and Elfarra (2012) noted that the  $\alpha,\beta$ -  
218 unsaturated sulfoxides formed in the GST pathway may be further conjugated with  
219 glutathione, but that this process could also be reversible (by retro-Michael addition).  
220 This would create a mechanism by which the reactive sulfoxides could circulate in a  
221 stabilized form through the blood to other organs where they may be regenerated. The  
222 mechanism would likely be operative for PCE as well.

223

#### 224 Pharmacokinetic Model

225 Numerous physiologically based pharmacokinetic (PBPK) models have been proposed  
226 for PCE over the course of several decades. Reddy (2005), Clewell (2005), and US EPA  
227 (2012a) have reviewed this body of research. Although the models are reasonably  
228 consistent in estimating PCE blood concentrations, they differ widely in their predictions  
229 of metabolized PCE at lower exposure concentrations. For example, at an inhaled  
230 concentration of 1 ppb, some models predict about 1 or 2 percent metabolism, while  
231 others predict metabolism in the range of 20 to 35 percent, and perhaps as high as 60  
232 percent (Chiu and Ginsberg, 2011). Since PCE's carcinogenic potency is likely to depend  
233 upon the formation of genotoxic metabolic products, the wide range of estimated PCE  
234 metabolism among models has been a recognized problem for assessing the cancer risk  
235 from low-level PCE exposure.

236

237 The most recent and comprehensive PBPK model for PCE is that of Chiu and Ginsberg  
238 (2011). It was developed following the recommendations of the National Research  
239 Council (NRC, 2010) that the available models for PCE be integrated into a single  
240 harmonized model incorporating various improvements. The Chiu and Ginsberg (2011)  
241 model incorporates lung, liver, kidney, fat, and venous blood compartments, and lumped  
242 compartments for rapidly and slowly perfused tissues. It has components for simulating  
243 inhalation, oral, and injection exposures. Absorption-desorption of PCE in the upper  
244 respiratory tract (i.e., the "wash-in/wash-out" effect) is also taken into account. The rate  
245 of PCE oxidation is modeled in liver, kidney and lung, and GSH conjugation is modeled  
246 in the liver and kidney. The model [can estimate \(for example\)s: concentrations of PCE in exhaled air, blood concentrations of PCE and TCA, blood concentrations](#) and urinary  
247 [excretion of TCA and the GSH-conjugation metabolites, N-AcTCVC and DCA. A](#)  
248 [graphical representation of the Chiu and Ginsberg PBPK model is provided in Figure 2.](#)

249

250  
251 [US EPA \(2012\) used the Chiu and Ginsberg \(2011\) model to estimate internal dose](#)  
252 [metrics in its recent PCE cancer potency factor update, which included the development](#)  
253 [of a URF for inhalation exposures.](#) The most important improvements of the Chiu and  
254 Ginsberg (2011) model, as discussed by the US EPA (2012a), are:

255

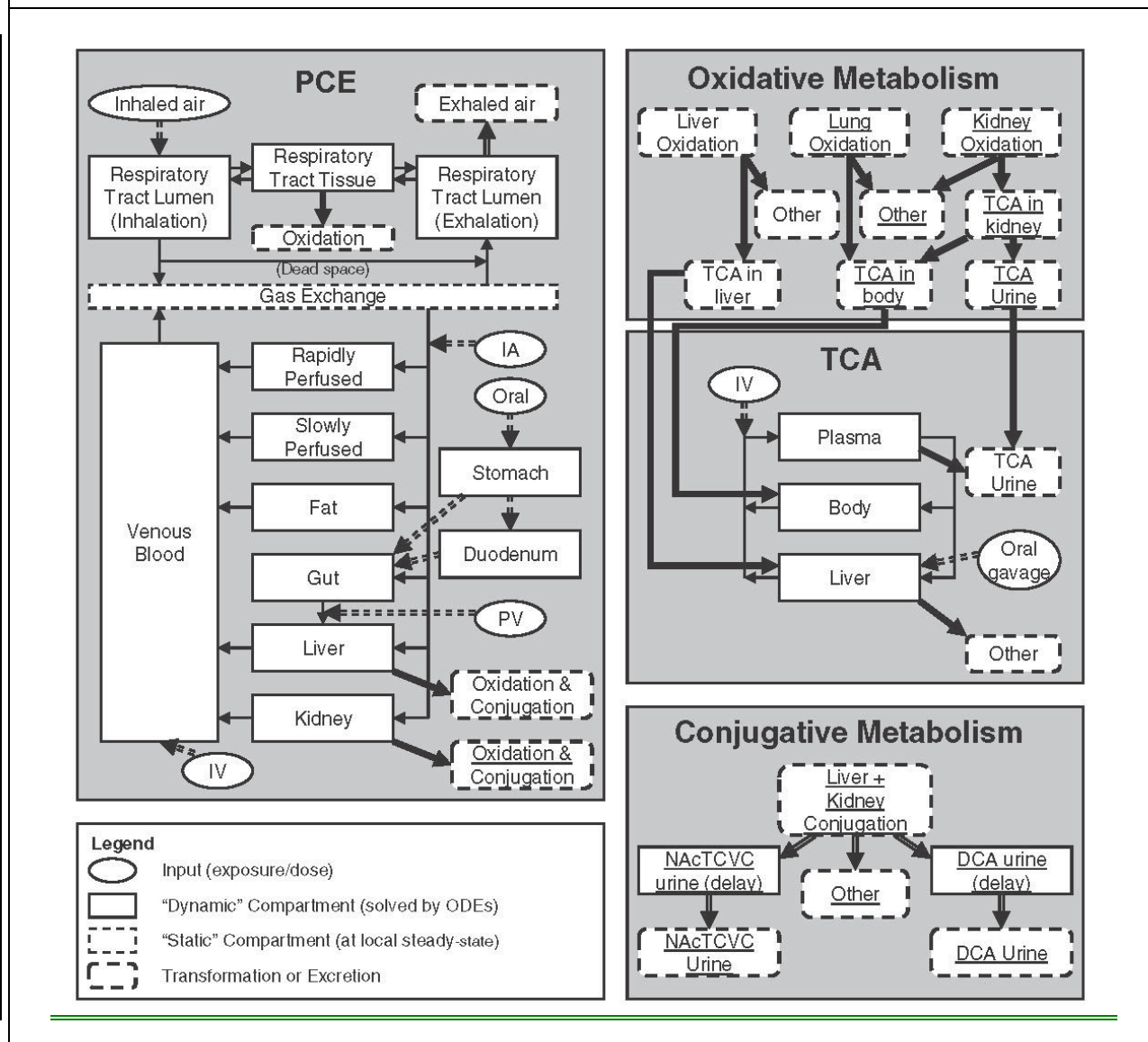
- 256 • It uses Bayesian Markov Chain Monte Carlo (MCMC) methodology to determine  
257 the most likely values (posterior modes) for key metabolic constants.
- 258 • The model utilized all the available toxicokinetic data for PCE in mice, rats, and  
259 humans, and is calibrated using a wide range of *in vivo* toxicokinetic data.

260

261  
 262  
 263  
 264  
 265

- It is the first model to include a separate glutathione conjugation pathway.
- It incorporates recent information on TCA toxicokinetics from trichloroethylene modeling studies.

**Figure 2: Chiu and Ginsberg (2011) PBPK Model for PCE (a)**



(a) Figure adapted from Chiu and Ginsberg (2011). IV = intravenous, IA = intra-arterial, PV = portal vein.

266  
 267  
 268  
 269

- It is the first model to include a separate glutathione conjugation pathway.
- It incorporates recent information on TCA toxicokinetics from trichloroethylene modeling studies.

270 [Chiu and Ginsberg \(2011\) used a hierarchical Bayesian population approach to obtain](#)  
271 [estimates of the posterior modes<sup>2</sup> for a subset of important PBPK model parameters](#)  
272 [including: the pulmonary ventilation rate, metabolic constants for oxidation and](#)  
273 [conjugation of PCE, and urinary excretion of metabolites. Other model parameters, such](#)  
274 [as partition coefficients and most of the physiological parameters, were fixed at baseline](#)  
275 [values chosen from the literature. Inclusion of several intake routes \(e.g., inhalation, oral,](#)  
276 [and intravenous\) allowed the model to be calibrated and evaluated against a wide variety](#)  
277 [of experimental \*in vivo\* data.](#)

278  
279 [In the MCMC analysis, sampling variation was characterized by running multiple chains](#)  
280 [of length 5000 \(retaining every 10th value\) using randomly chosen starting conditions for](#)  
281 [each chain. For the rodent PBPK models, 24 independent MCMC chains were run, each](#)  
282 [producing a chain-specific, posterior mode estimate. The parameter set with highest](#)  
283 [overall posterior probability of all the chains was selected as the posterior mode of the](#)  
284 [optimized PBPK model. For the human model, 48 independent chains were used since](#)  
285 [preliminary analysis indicated a potential for multiple maxima.](#)

286  
287 [Table 1 shows a summary of model predictions for several types of dose metrics based](#)  
288 [on the optimized model for inhalation exposures, as reported by Chiu and Ginsberg](#)  
289 [\(2011\). With respect to the prediction range of the dose-metric estimates was narrow for](#)  
290 [both the PCE AUC and PCE oxidation metrics, the range of chain-specific values was -](#)  
291 [less than 40% of the overall posterior mode estimates \(<20%\). For example, in the](#)  
292 [mouse model at 1 ppm exposure, the overall posterior mode for percent of PCE oxidized](#)  
293 [was 17.4% of intake, and the range of chain-specific posterior modes was 11.5% to](#)  
294 [17.9%.<sup>3</sup> and oxidation \(<1.5 fold\). In contrast, t](#)

295  
296 [The estimates for PCE conjugation were more variable \(with the exception of the rat](#)  
297 [model\). In mice exposed at 1 ppm, for example, the model predicts that 0.016% of PCE](#)  
298 [intake will be conjugated with a range of 0.0068% to 0.43%. In the human model, the](#)  
299 [overall posterior mode indicates that 9.4% of PCE intake is metabolized by GSH](#)  
300 [conjugation, with a range of 0.003% to 10%. he dose metrics for the GST pathway in](#)  
301 [humans and mice displayed significantly larger variability. In the human model](#)  
302 [displayed, the MCMC analysis produced an apparently bimodal distribution for the rate](#)  
303 [of GSH conjugation, with an approximately 3000 fold difference between the two](#)  
304 [highest likelihood, posterior modes. Nonetheless, the most probable posterior mode -](#)  
305 [\(i.e., the maximum likelihood estimate, or "MLE"\) was at the high end of estimated](#)  
306 [conjugation rates in humans. For example, the MLE indicates that humans will](#)  
307 [conjugate 9.4 percent of PCE intake with posterior mode estimates ranging from 3.2E-03](#)  
308 [to 10 percent.](#)

309  
310 [In mice, the range of posterior modes for GSH conjugation was approximately 60-fold.](#)  
311 [However, in this case, the MLE was closer to the low end of the MCMC-estimated](#)  
312 [values. For example, for mice exposed to 1 ppm PCE, the MLE indicates that 0.016-](#)

<sup>2</sup> These are also the maximum likelihood estimates (MLEs) since flat prior distributions were used in the model.

<sup>3</sup> Ranges of MCMC chain-specific posterior modes are from Table S-8 of Chiu and Ginsberg, 2011

313 ~~percent of intake will be conjugated, while the range of posterior modes is 0.0068 to 0.43~~  
314 ~~percent (from Table S-8 of Chiu and Ginsberg, 2011).~~

315  
316 ~~Regarding GSH conjugation in humans,~~ Chiu and Ginsberg (2011) were not able to  
317 determine how much of the spread in the human conjugation model was due to ~~model~~  
318 uncertainty or population variation, but noted that the distribution could represent actual  
319 variability given the large differences in GST activities displayed by humans. On the  
320 other hand, a high level of variability was not observed in metabolic studies of  
321 trichloroethylene (TCE). Lash *et al.* (1999) looked at rates of GSH conjugation of TCE in  
322 40 ethnically and age-diverse, male and female human liver samples and found less  
323 than a 10-fold variation.

324  
325 As noted above, US EPA (2012a) used Chiu and Ginsberg's model results to derive its  
326 updated PCE potency factors. However, because of the large range of model estimates  
327 for PCE conjugation, US EPA prioritized the dose metrics based on oxidative metabolism  
328 and PCE AUC in their final analysis.  
329 \_\_\_\_\_

<u>Table 1: PCE Internal Dose Metrics from the Chiu and Ginsberg (2011) PBPK Model (and reproduced by the OEHHA model extract) <sup>(a)</sup></u> <i>Constant Inhalation Doses (posterior mode estimates)</i>						
<u>Dose metric</u>	<u>Exposure Concentration (ppm)</u>					<u>Prediction Range (at 1 ppm)</u>
	<u>0.01</u>	<u>1</u>	<u>10</u>	<u>100</u>	<u>1000</u>	
<u>PCE AUC Blood</u>	<i>(mg-hr)/(L-d) per ppm</i>					
<u>Mouse</u>	<u>2.1</u>	<u>2.2</u>	<u>2.4</u>	<u>2.6</u>	<u>2.7</u>	<u>2.2-2.4</u>
<u>Rat</u>	<u>2.25</u>	<u>2.25</u>	<u>2.25</u>	<u>2.25</u>	<u>2.4</u>	<u>2.25-2.27</u>
<u>Human</u>	<u>2.0</u>	<u>2.0</u>	<u>2.0</u>	<u>2.0</u>	<u>2.0</u>	<u>2.0-2.4</u>
<u>PCE Oxidation</u>	<i>Percent of intake that is oxidized</i>					
<u>Mouse</u>	<u>18.8</u>	<u>17.4</u>	<u>11.8</u>	<u>7.3</u>	<u>6.6</u>	<u>11.5-17.9</u>
<u>Rat</u>	<u>4.2</u>	<u>4.2</u>	<u>4.1</u>	<u>3.3</u>	<u>1.1</u>	<u>3.9-4.2</u>
<u>Human</u>	<u>0.98</u>	<u>0.98</u>	<u>0.98</u>	<u>0.98</u>	<u>0.98</u>	<u>0.69-1.0</u>
<u>PCE Conjugation</u>	<i>Percent of intake that is conjugated</i>					
<u>Mouse</u>	<u>0.015</u>	<u>0.016</u>	<u>0.021</u>	<u>0.025</u>	<u>0.026</u>	<u>0.0068-0.43</u>
<u>Rat</u>	<u>0.31</u>	<u>0.31</u>	<u>0.31</u>	<u>0.32</u>	<u>0.335</u>	<u>0.20-0.50</u>
<u>Human <sup>(b)</sup></u>	<u>9.4</u>	<u>9.4</u>	<u>9.4</u>	<u>9.4</u>	<u>9.3</u>	<u>0.003-10.0 (bimodal) <sup>(b)</sup></u>

(a) Values are from Chiu and Ginsberg (2011), Tables S-6 through S-8, and are also reproduced by OEHHA's inhalation-only model extract, at the presented level of significance.

(b) Values presented are for the most probable posterior mode.

330

331 Use of Chiu and Ginsberg (2011) Harmonized PBPK Model

332 Although there are unresolved issues related to the Chiu and Ginsberg model predictions  
333 for PCE's GST pathway, OEHHA considers the model to be the best available  
334 methodology for estimating dose metrics in the dose-response assessment. Regarding  
335 uncertainty in GSH conjugation, the Office evaluated the effect of including the GST  
336 pathway in the dose metric on the overall cancer potency analysis (see the following  
337 section).

338

339 ~~As the following section will demonstrate, the impact of uncertainty in the human GSH-~~  
340 ~~conjugation rate is significantly muted when both PCE oxidation and GSH conjugation-~~  
341 ~~are included together as a total metabolized dose in the dose-response calculations.~~

342

343 The full Chiu and Ginsberg (2011) model contains large portions of code designed to  
344 perform the Bayesian MCMC simulation, which determined the posterior mode estimates

345 for key PBPK parameters. Once obtained, the posterior modes can be used to forecast  
346 the most likely values for internal doses at various exposure concentrations.

347  
348 ~~OEHHA~~ For the inhalation potency evaluation, OEHHA relied on Chiu and Ginsberg's  
349 optimized PBPK model results. Since only dose metrics for inhalation exposures needed  
350 to be estimated, the inhalation-relevant portion of the Chiu and Ginsberg (2011) model  
351 was extracted. Specifically, OEHHA: (1) identified ~~ing~~ the main inhalation components of  
352 the MC-Sim program obtained from the authors, (2) extracted ~~ing~~ the relevant equations  
353 and ~~inputs input parameters~~ from the model code and translated ~~ing~~ them from the MC-  
354 Sim language into Berkeley Madonna code, (3) ran ~~running~~ the ~~pared-down code~~ using  
355 the optimized, Bayesian posterior mode parameters and other baseline values  
356 developed by Chiu and Ginsberg (2011) in the usual deterministic manner, and (4)  
357 tested ~~ing~~ the output against the original model ~~dose estimates estimates~~ reported in the  
358 Chiu and Ginsberg (2011) paper.  
359 ~~. The optimized, Bayesian posterior mode parameters and other baseline values~~  
360 ~~developed by Chiu and Ginsberg (2011) were used in the adapted model.~~

361  
362 A graphic depicting OEHHA's inhalation-only model is presented in Figure 3. As in the  
363 original Chiu and Ginsberg model, it includes lung, liver, kidney, fat, and venous blood  
364 compartments, and lumped compartments for rapidly and slowly perfused tissues. The  
365 first transformation in the oxidative pathway is modeled in the lung, liver, and kidney, and  
366 the first step of the GST pathway is included for liver and kidney. Absorption-desorption  
367 of PCE in the upper respiratory tract is also included. The model adequately reproduced  
368 the predictions of the original Chiu and Ginsberg model for inhalation exposures:  
369 OEHHA's model extract reproduces the internal dose-metric values obtained by Chiu  
370 and Ginsberg (2011), as presented in Table 1. The Berkeley Madonna model code for  
371 mouse, rat, and human is provided in Appendix A.

### 372 *Uncertainty and/or Variation in the Model Estimates*

374 Additional discussion of the uncertainty related to GSH conjugation, particularly in the  
375 human model, is provided here to support the choice of dose metric (presented later, in  
376 Section 9). Three issues are addressed as follows.

377  
378 First, as noted above, the modeled rate of GSH conjugation in humans displayed a  
379 relatively high amount of uncertainty and/or variation: 0.003 -10%, with the overall  
380 posterior mode at 9.4% of intake. Commenting on this large range, Chiu and Ginsberg  
381 (2011) noted that the *in vivo* data available for model calibration were "inadequate to  
382 constrain the flux through this pathway, either extreme providing plausible fits to the  
383 data."

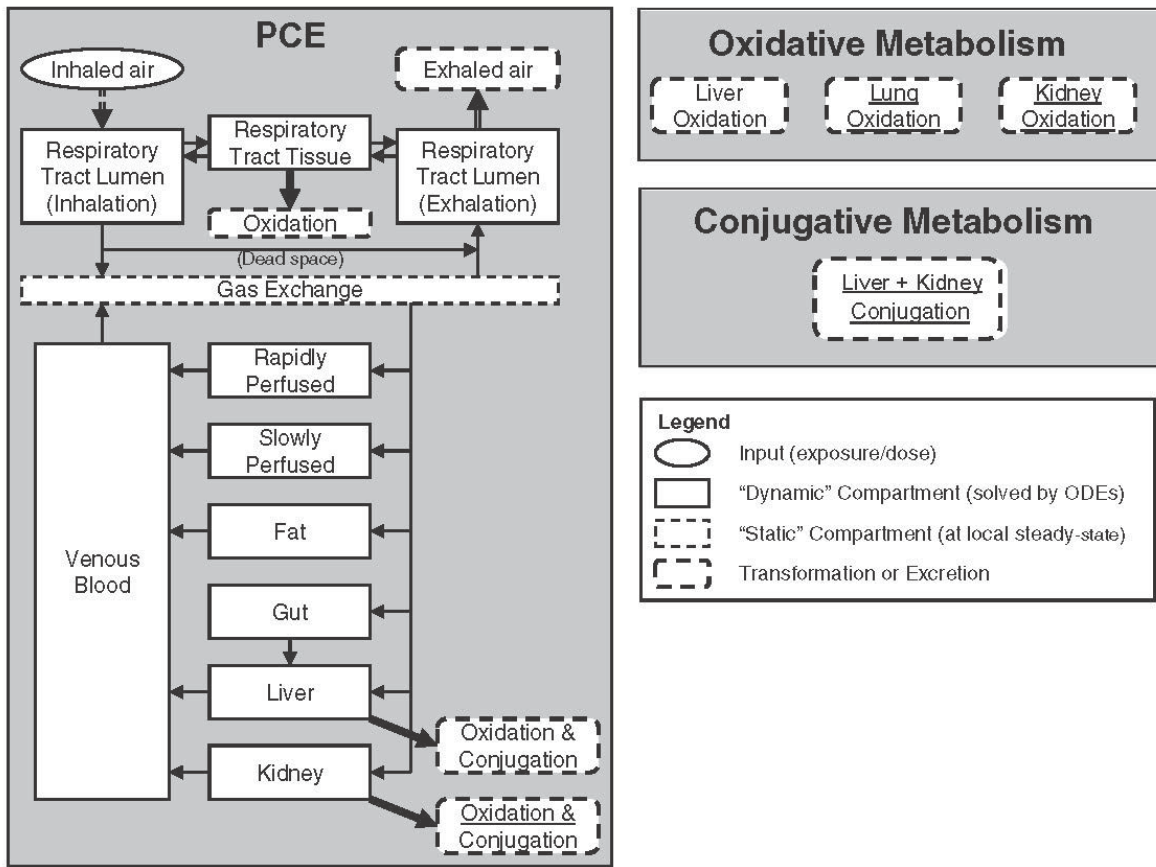
384  
385 The overall posterior mode for PCE conjugation is, however, consistent with the *in vitro*  
386 rates for TCE and other halogenated VOCs that have been reported in the literature  
387 (e.g., Lash *et al.*, 1998; and Wheeler, *et al.*, 2001). The low value for PCE conjugation is  
388 consistent with the low-end of *in vitro* activity obtained for PCE by Dekant *et al.* (1998),

389 | which were below the analytical method detection limits.<sup>4</sup>  
390 | \_\_\_\_\_

---

<sup>4</sup> It should be noted that the *in vitro* GSH-conjugation data was not used to calibrate the model.

**Figure 3: Inhalation-Only PBPK Model for PCE <sup>(a)</sup>**



(a) Figure adapted from Chiu and Ginsberg (2011).

**Table 1: PCE Internal Dose Metrics from the Chiu and Ginsberg (2011) PBPK Model (and OEHHA Adapted Model)<sup>(a)</sup>**

*Constant Inhalation Dose (posterior mode estimates)*

Dose metric	Exposure Concentration (ppm)				
	Prediction Range				
	0.01	1	10	100	
<i>PCE AUC Blood</i>	<i>(mg-hr)/(L-d) per ppm</i>				
Mouse	2.4	2.4	2.4	2.6	<10%
Rat	2.25	2.25	2.25	2.25	<10%
Human	2.0	2.0	2.0	2.0	<20%
<i>PCE Oxidation</i>	<i>Percent of intake that is oxidized</i>				
Mouse	18.8	17.4	11.8	7.3	<40%
Rat	4.2	4.2	4.1	3.3	<20%
Human	0.98	0.98	0.98	0.98	<1.5-fold
<i>PCE Conjugation</i>	<i>Percent of intake that is conjugated</i>				
Mouse	0.015	0.016	0.021	0.025	~60-fold
Rat	0.31	0.31	0.31	0.32	<30%
Human	9.4	9.4	9.4	9.4	~3000-fold

(a) Values are from Chiu and Ginsberg (2011), Tables S-6 through S-8, and are also reproduced by OEHHA's inhalation-only model adaptation, at the presented level of significance.

(b) Values are presented for higher probability, upper mode.

392 The large prediction range obtained in the human conjugation model raises a question -  
 393 particularly with regard to interspecies dose extrapolation - of whether the model's GSH  
 394 conjugation estimates should be used along with the PCE oxidation rates in a "total  
 395 metabolized dose" metric. The alternative would be to define an internal dose metric  
 396 using only the less-variable model predictions for PCE oxidation, as was done by US  
 397 EPA (2012a).<sup>5</sup>

398  
 399 The impact of PBPK model uncertainty in this case is muted when both PCE oxidation  
 400 and GSH conjugation are included together as a total metabolized dose, increasing the  
 401 potency estimate by about one order of magnitude (much less than the range observed  
 402 in the MCMC analysis).

403  
 404 In order to demonstrate this, OEHHA compared the results of interspecies dose  
 405 extrapolation using the human PBPK model with the two alternative dose metrics, i.e.,

<sup>5</sup> Omitting GSH-conjugation from the internal dose metric is similar to using the lower-likelihood mode for human GSH-conjugation in a total metabolized dose. ~~since, w~~With the lower mode, the rates of conjugation for humans, rats, and mice would all be small relative to PCE oxidation rates, and thus have little impact on both the dose-response calculations using the rodent data and interspecies dose extrapolation using the human PBPK model.

406 using either total metabolism (GSH-conjugation + PCE oxidation) or PCE oxidation-only  
407 metabolism. We used the model to calculate human equivalent concentrations (HECs)  
408 from a range of example benchmark doses that could be obtained from the dose-  
409 response modeling of PCE exposure in rodents. As can be seen from the PBPK-derived  
410 HEC values presented in Table 2, the total metabolism dose metric produces HECs that  
411 are about 11-fold OEHHA's inhalation-only adaptation of the Chiu and Ginsberg (2011)-  
412 model includes lung, liver, kidney, fat, and venous blood compartments, and lumped  
413 compartments for rapidly and slowly perfused tissues. The first transformation in the  
414 oxidative pathway is modeled in the lung, liver, and kidney, and the first step of the GST  
415 pathway is included for liver and kidney. Absorption-desorption of PCE in the upper  
416 respiratory tract is also included. The model adequately reproduced the predictions of  
417 the original Chiu and Ginsberg model for inhalation-only exposures. The Berkeley  
418 Madonna model code for mouse, rat, and human is provided in Appendix A.

419  
420 *Uncertainty and/or Variation in the Model Estimates*

421 Additional discussion of the modeling uncertainty related to GSH conjugation, particularly  
422 in the human model, is provided here to support the choice of dose metric (presented  
423 later, in Section 9). Three issues are addressed as follows.

424  
425 First, as noted above, the modeled rate of GSH conjugation in humans produced an  
426 apparently bimodal distribution with an approximately 3000-fold difference between the  
427 two highest likelihood posterior modes. The higher-likelihood mode (i.e., MLE) predicts  
428 PCE-conjugation levels that are consistent with the high range of *in vitro* estimates for  
429 conjugation of TCE and other halogenated VOCs that have been reported in the  
430 literature (e.g., Lash *et al.*, 1998; and Wheeler, *et al.*, 2001). The lower-likelihood mode  
431 predicts levels of PCE conjugation consistent with the low-end of *in vitro* enzyme  
432 activities obtained for PCE by Dekant *et al.* (1998), which were below the analytical  
433 method detection limits.

434  
435 The large range of uncertainty in the human model raises a question—particularly with  
436 regard to interspecies dose extrapolation—of whether the model's GSH conjugation  
437 predictions should be used along with the PCE oxidation rates in a "total metabolized  
438 dose" metric. The alternative would be to define an internal dose metric using only the  
439 less-variable model predictions for PCE oxidation.

440  
441 A comparison of interspecies dose extrapolation using these two alternative dose metrics  
442 indicates that the 3000-fold range in predicted human GSH conjugation rates does not  
443 produce a similarly large range of possible outcomes in the dose extrapolation  
444 calculation. Indeed, the human equivalent concentrations (HECs) obtained by  
445 extrapolating total metabolized doses are only about one order of magnitude larger than  
446 the smaller than HECs that would be obtained by using an oxidation-only dose metric.<sup>6</sup>

---

<sup>6</sup>Omitting the GSH-conjugation component from the internal dose metric is similar to using the lower-likelihood mode for human GSH conjugation in a total metabolized dose since, with the lower mode, the rates of conjugation for humans, rats, and mice would all be small relative to PCE oxidation rates, and thus have little impact on both the dose-response calculations using the rodent data and interspecies dose extrapolation using the human PBPK model.

447 [\(Note that smaller HECs result in larger cancer potency factors\). This is readily seen by](#)  
 448 [using the PBPK model to calculate HECs for a relevant range of metabolized doses for](#)  
 449 [each dose metric. Model results are provided in Table 2 below.](#)  
 450

Table 2: Impact of Internal Dose Metric Choice on Interspecies Conversion Calculations			
Example Rodent Benchmark Metabolized Doses <sup>(a)</sup> (mg/kg-d)	PBPK-Derived <a href="#">Human Equivalent Concentration</a> (HEC <sub>i</sub> (ppm))		Ratio of HECs
	Oxidative + GSH Conjugation	Oxidative Metabolism Only	
0.01	0.061	0.65	10.7
1.0	6.1	65.0	
3.0	18.2	195.0	

(a) [Note that since oxidative metabolism is significantly greater than GSH conjugation in rodents, both dose metrics will produce similar benchmark doses in the rodent dose-response models. A rough HEC comparison can therefore be made on a single benchmark metabolized dose for both dose-metric scenarios.](#)

451 [Thus, it appears that using a dose-metric incorporating a "high-end" value for human](#)  
 452 [GSH conjugation, as opposed to using an oxidation-only dose metric which effectively](#)  
 453 [sets GSH-conjugation to zero, adds a relatively small amount of "conservatism" to the](#)  
 454 [dose-response analysis. OEHHA has determined that inclusion of the GST pathway in a](#)  
 455 [total metabolized dose metric ensures that the resulting potency values are adequate to](#)  
 456 [protect public health, per the recommendations of our current Air Toxics Hotspots](#)  
 457 [program risk assessment guidelines \(OEHHA, 2009\).](#)  
 458

459 A second issue is whether using the model's uncertain estimate for glutathione  
 460 conjugation in mice could have a large impact upon the dose-response calculation. As  
 461 above, this question is addressed by looking at the difference between using either total  
 462 metabolism or oxidation-only metabolism as the dose metric. In this case, the impact  
 463 would be low. From Table 1, the model's [posterior mode MLE](#) estimates of PCE  
 464 oxidation and conjugation in mice indicate that oxidation dominates conjugation by  
 465 factors of 290-1250, such that both dose metrics (total and oxidation-only) reflect mainly  
 466 PCE oxidation, and should produce similar benchmark doses in a dose-response model.  
 467

468 Finally, there is an unresolved disagreement regarding the large variation in the results  
 469 of key *in vitro* studies that have estimated glutathione conjugation of PCE and TCE in  
 470 rodent and human tissues. In its IRIS PCE review, the US EPA (2012a) pointed out:

471  
 472 "The GSH pathway for tetrachloroethylene was originally demonstrated only in  
 473 rodents, and interpretation of the then-existing data led some scientists to  
 474 conclude that the pathway was not operative in humans (Green *et al.*, 1990).  
 475 More recent data clearly demonstrate the existence of the pathway in humans

476 (Schreiber *et al.*, 2002; Völkel *et al.*, 1998; Birner *et al.*, 1996) [...]

477  
478 "There are discrepancies regarding reported rates of tetrachloroethylene GSH  
479 metabolism (Lash *et al.*, 2007; Lash and Parker, 2001; Dekant *et al.*, 1998; Lash  
480 *et al.*, 1998; Green *et al.*, 1990). These differences may be due, in part, to  
481 different chemical assay methodology or to problems resulting from the stability of  
482 the chemical product being measured or both (Lash and Parker, 2001)."

483  
484 Some of the *in vitro* studies predict relatively higher-TCVG (and DCVG) production rates  
485 in humans ~~than in rodents~~ (e.g., Lash *et al.*, 1998; Lash *et al.*, 1999), while others appear  
486 to predict indicate very low conjugation. that humans produce much less TCVG (and  
487 DCVG) than rodents. For example, with TCE, Green *et al.* (1997) measured DCVG  
488 formation at 0.19 picomole per minute per milligram protein (pmol/min/mg) using human  
489 liver cytosol from 4 individuals. Conversely, Lash *et al.* (1999) measured TCE  
490 conjugation at 5,770 (pmol/min/mg) in human cytosolic protein pooled from 20  
491 individuals. This large difference in measured GSH conjugation rates is reflected in the  
492 uncertainty/variability displayed by the Chiu and Ginsberg human model (and to a lesser  
493 extent, the mouse model).

494  
495 Several commentators have raised doubts regarding the accuracy of the PCE and TCE  
496 conjugation rates reported by Lash *et al.* (1998, 1999, 2007), pointing to potential issues  
497 with the chemical analysis methods used by the laboratory. On the other hand, the  
498 apparent chemical instability of the GSH conjugates raises questions for studies that  
499 have measured low conjugate levels. However, no work has apparently been done to  
500 determine the true source of the discrepancy among the various divergent study results.  
501 The Lash laboratory has published several papers following Lash *et al.* (1998) involving  
502 the analysis of TCVG and DCVG, and has described various quality controls used  
503 ensure analytical accuracy.<sup>7</sup> Consistent results were generally obtained in these studies.  
504 On the other hand, Lash, *et al.* (2006) measured DCVG levels in blood and tissue  
505 samples of rats orally exposed to TCE and obtained a mixture of high and unexpectedly  
506 low values. However, the higher values obtained by Lash *et al.* (2006) were generally  
507 consistent with blood DCVG concentrations found in orally exposed mice by Kim *et al.*  
508 (2009), and with mouse tissue and serum concentrations measured by Yoo, *et al.*  
509 (2015), both using a different method of analysis.

510  
511 Discrepancies in measured conjugation rates in humans might also be due to variable  
512 quality of the tissue samples used, and it is possible that some samples were not  
513 representative of the known variation in human GST activities. Thus, OEHA does not  
514 find convincing evidence to discount the high-end *in vitro* values for human glutathione  
515 conjugation of PCE, and estimated by the Chiu and Ginsberg (2011) PBPK model as  
516 well.

517  
518

---

<sup>7</sup> For example see, Lash *et al.* (2007) and Lash, *et al.* (1999).

519 **7. GENOTOXICITY AND CARCINOGENICITY**

520 Genotoxicity

521 A large number of studies have tested the genotoxicity of PCE, and less frequently its  
522 metabolites, in microorganisms, mammalian cells, and in *Drosophila* and rodents. There  
523 have also been a few occupational exposure studies looking at genetic abnormalities in  
524 lymphocytes. This literature has recently been reviewed in detail by IARC (2014) and  
525 US EPA (2012a). Selected results based on these reviews and the literature are  
526 presented below.

527  
528 PCE was not mutagenic in the Ames test with *S. typhimurium* or *E. coli* in the presence  
529 or absence of S9 metabolic activation. It was mutagenic, however, in *S. typhimurium*  
530 when tested with purified rat-liver GST, glutathione, and rat kidney fractions, where  
531 TCVG would be formed (Vamvakas, *et al.*, 1989). Most studies looking at chromosomal  
532 aberrations, micronuclei formation, or sister chromatid exchange have been negative,  
533 but micronuclei induction was seen in Chinese hamster ovary cells (Wang *et al.*, 2001)  
534 and human lymphoblastoid cells expressing CYP450 enzymes (White *et al.*, 2001).  
535 Genetic alterations have also been observed in rapidly growing yeast cell cultures (US  
536 EPA, 2012a).

537  
538 Other types of tests, such as DNA strand break assays, DNA adduct and cell  
539 transformation studies, and *Drosophila* mutation tests have provided mixed results.  
540 Positive findings include: Elevated DNA single-strand breaks in mouse liver and kidney  
541 *in vivo* (Walles, 1986), and DNA-adduct formation in mouse and rat tissues *in vivo*  
542 (Mazzullo, *et al.*, 1987).

543  
544 Results from occupational studies have also been mixed. Ikeda *et al.* (1980) tested ten  
545 factory workers exposed to high (92 ppm PCE) or low (10-40 ppm) and found no  
546 evidence of cytogenetic damage to lymphocytes or altered cell cycle kinetics. No  
547 increase in sister chromatid exchanges in lymphocytes was found in a study of 27  
548 subjects exposed to 10 ppm (geometric mean) of PCE (Seiji *et al.*, 1990). A decrease  
549 (not increase) of 8-hydroxy-deoxyguanosine, a marker of oxidative DNA damage, was  
550 observed in leukocytes of 38 female dry cleaners exposed to average concentrations of  
551 less than 5 ppm PCE (Toraason *et al.*, 2003). On the other hand, a study of 18 dry-  
552 cleaning workers exposed to 3.8 ppm PCE (average) found evidence of short-term  
553 genetic damage to peripheral blood lymphocytes, indicated by an increase in acentric  
554 chromosomal fragments (Tucker *et al.*, 2011).

555  
556 Genotoxicity testing of various PCE metabolites includes the following positive results:

- 557
- 558 • TCA exhibited genotoxicity in several *in vivo* tests, for example: DNA strand  
559 breaks, chromosomal abnormalities, and micronucleus formation in mice; and  
560 chromosomal aberrations in chicken bone marrow (IARC, 2014; US EPA,  
561 2012a).
  - 562 • Genotoxicity has been demonstrated with DCA in the Ames test, micronucleus  
563 induction test, a mouse lymphoma assay, and *in vivo* cytogenetic tests; DCA has

- 564 also been shown to cause DNA strand breaks *in vivo* in mouse and rat liver  
565 (*ibid.*).
- 566 • Trichloroacetyl chloride vapor tested positive in the Ames test with and without  
567 metabolic activation (DeMarini, *et al.*, 1994).
  - 568 • PCE epoxide was mutagenic without metabolic activation in the Ames test with  
569 *S. typhimurium* TA1535 at the lower doses tested; toxicity occurred at higher  
570 doses (Kline *et al.*, 1982).
  - 571 • TCVG incubated with rat kidney protein containing  $\gamma$ -glutamyl transpeptidase  
572 (GGT) and dipeptidases was mutagenic in the Ames test (Vamvakas, *et al.*,  
573 1989).
  - 574 • TCVC and N-AcTCVC tested positive in the Ames test without metabolic  
575 activation (Dekant *et al.*, 1986; Vamvakas, *et al.*, 1987).
  - 576 • TCVC sulfoxide was mutagenic in the Ames test with *S. typhimurium* TA 100, but  
577 was 30-fold less potent than TCVC (Irving and Elfarra, 2013).

578  
579 In addition, several metabolites have been tested for carcinogenicity in animals. Dermal  
580 exposure of mice to PCE epoxide induced skin tumors (Van Duuren, *et al.*, 1983).  
581 Several long-term drinking-water bioassays of TCA and DCA in mice, with limited  
582 pathologic analysis of tissues other than the liver, found increases in hepatocellular  
583 tumors. Initiation–promotion studies with TCA or DCA in mice also demonstrated that  
584 they promote liver tumors following initiation by other carcinogens (IARC, 2014; Guyton  
585 *et al.*, 2014).

586  
587 Cancer Epidemiology

588 Numerous epidemiologic studies of PCE have been published, including more than 25  
589 larger cohort and case-control studies since OEHHA's last toxicity review (*circa* 2000,  
590 for our PHG for drinking water). Several detailed reviews of the literature have recently  
591 been published (Guyton, *et al.*, 2014; IARC, 2014; and US EPA, 2012a).

592  
593 Epidemiologic studies of PCE have all relied on semi-quantitative measures of exposure  
594 such as high/medium/low, ever/never exposed, or job categories. As such, the exposure  
595 data in this body of research are not of sufficient quality for use in quantitative dose-  
596 response analysis. However, it provides evidence that PCE causes cancer in humans  
597 and qualitatively supports the development of a unit risk value from animal studies. US  
598 EPA (2012a) evaluated the results of the cohort and case-control studies that  
599 developed more precise exposure assessments and concluded that PCE increases the  
600 risk of three types of cancer in humans: bladder cancer, non-Hodgkin's lymphoma  
601 (NHL), and multiple myeloma. IARC (2014) agreed with US EPA regarding bladder  
602 cancer, but concluded that the evidence for PCE inducing other cancers in humans was  
603 insufficient given the conflicting results across various studies. With non-Hodgkin's  
604 lymphoma, for example, "three cohort studies showed an increased risk based on small  
605 numbers, and the largest study with the best control of potential confounders did not.  
606 Case-control studies on non-Hodgkin lymphoma did not find significant associations"  
607 (*ibid.*).

608

609 A recent meta-analysis of bladder cancer risk in dry-cleaning workers (Vlaanderen, *et*  
610 *al.*, 2014) integrated the results of seven studies and 139 exposed cases, and found an  
611 overall relative risk level of about 1.5 for exposed versus non-exposed groups (with a  
612 95% confidence level of 1.16 to 1.85).

613

614 *Animal Studies of PCE*

615 Increased tumor incidence was found in mice and rats in three long-term carcinogenicity  
616 studies of PCE. An oral study was conducted by the National Cancer Institute  
617 (NCI, 1977), where B6C3F<sub>1</sub> mice and Osborne-Mendel rats were administered PCE in  
618 corn oil by gavage, 5 days/week for 78 weeks with additional follow-up of 32 weeks for  
619 rats and 12 weeks for mice. PCE caused a significant increase of hepatocellular  
620 carcinomas in mice of both sexes, and the tumors appeared considerably sooner in  
621 treated mice than in controls. Survival in the high dose groups was much lower than the  
622 control group at 40 to 45 weeks, and toxic nephropathy was observed in 93% of mice  
623 exposed. In rats, a high level of early mortality occurred in all treated groups, which  
624 obscured conclusions regarding carcinogenicity.

625

626 Two lifetime inhalation bioassays of PCE have also been published and are described  
627 as follows.

628

629 A lifetime inhalation cancer study was conducted by the Japan Bioassay Research  
630 Center (JBRC) of the Japan Industrial Safety and Health Association (JISHA, 1993).  
631 Good Laboratory Practice (GLP) standards were used in the conduct of the study.  
632 Dose-response data was analyzed by standard statistical procedures and study results  
633 were thoroughly documented in a manner similar to NTP rodent cancer study reports.

634

635 The study was conducted using F344/DuCrj rats and Crj:BDF<sub>1</sub> mice. Groups of 50 male  
636 and 50 female rats were exposed to PCE (99.0% pure) at 50, 200 or 600 ppm, and  
637 similar groups of mice were exposed to 10, 50, or 250 ppm, for 6 hours per day, 5 days  
638 per week, and 104 weeks. During the study period, the general status, body weight, and  
639 food consumption of the animals were monitored. Urinalyses, hematological, and blood  
640 chemistry tests were performed near the end of exposure for the surviving animals.  
641 Upon death, animals were necropsied and organ weights were determined.  
642 Histopathologic examination of all major tissue types was performed on all animals.  
643 Survival was good for both sexes of rats and mice in all dose categories: more than 80  
644 percent of rats and 70 percent of mice were alive at week 92. Nonetheless, survival was  
645 significantly reduced at the highest exposure levels when compared with control groups.  
646 Additional findings related to tumorigenesis are (see also Table 3):

647

- 648 • For exposed male and female rats, the only tumor type that was found to be  
649 elevated was mononuclear cell leukemia (MCL). A statistically significant dose-  
650 response trend was found by the Cochran-Armitage and exact trend tests (in  
651 males) or a life-table test (in females). In addition, for males, the highest dose  
652 category displayed a significant increase when compared to controls by the  
653 Fisher exact test.

654

655

656

657

658

659

- In exposed mice, an increased incidence of hepatocellular adenoma and carcinoma was found in both sexes as indicated by significant dose-response trends and pair-wise comparison of the high dose category against controls. In the males, there was also an increase in all-organ, hemangioma or hemangiosarcoma (mostly in the spleen and liver), and Harderian gland tumors.

<b>Table 3: Primary Tumor Incidence in Mice and Rats Exposed to PCE Rates at Exposure Concentrations in PPM (JISHA, 1993)</b>									
<b>Mice (Crj:BDF<sub>1</sub>)</b>									
Tumor Type	Sex	Adjusted Rates <sup>(a)(b)</sup> (at 0-250 ppm)				Rate Percent (at 0-250 ppm)			
		0	10	50	250	0	10	50	250
Hepatocellular adenoma or carcinoma	M	13/46**	21/47	19/47	40/49**	28.3	44.7	40.4	81.6
	F	3/44**	3/41	7/40	33/46**	6.8	7.3	17.5	71.7
Hemangioma or hemangiosarcoma (All sites)	M	4/46*	2/47	7/47	9/49*	8.7	4.3	14.9	18.4
Harderian gland adenoma	M	2/41**	2/45	2/37	8/39	4.9	4.4	5.4	20.5

<b>Rats (F344/DuCrj)</b>									
Tumor Type	Sex	Adjusted Rates <sup>(a)(b)</sup> (at 0-600 ppm)				Rate Percent (at 0-600 ppm)			
		0	50	200	600	0	50	200	600
Mononuclear cell leukemia	M	11/50**	14/48	22/50	27/49*	22.0	29.2	44.0	55.1
	F	10/50 <sup>(c)</sup>	17/50	16/50	19/50	20.0	34.0	32.0	38.0

(a) Tumor-incidence denominator adjusted by excluding animals dying before the first corresponding tumor type observed in each study.

(b) Statistical test indicators: (\*) P-value < 0.05; (\*\*) P-value < 0.005. Fisher exact test results are as reported by JISHA, except that mouse, all-site hemangioma/hemangiosarcoma values were calculated by OEHHA. The control group column indicates the results of trend tests. Both the Cochran-Armitage trend test (reported by JISHA) and the exact trend test calculated by OEHHA gave the same indications of significance.

(c) A significant trend was found in a life-table test reported by JISHA, P-value = 0.049.

<b>Table 4: Primary Tumor Incidence in Mice and Rats Exposed to PCE Rates at Exposure Concentrations in PPM (NTP, 1986)</b>							
<b>Mice (B6C3F<sub>1</sub>)</b>							
Tumor Type	Sex	Adjusted Rates <sup>(a)(b)</sup> (at 0-200 ppm)			Rate Percent (at 0-200 ppm)		
		0	100	200	0	100	200
Hepatocellular adenoma or carcinoma	M	17/49**	31/47**	41/50**	34.7	70.0	82.0
	F	4/44**	17/42**	38/47**	9.1	40.5	80.9

<b>Rats (F344/N)</b>							
Tumor Type	Sex	Adjusted Rates <sup>(a)(b)</sup> (at 0-400 ppm)			Rate Percent (at 0-400 ppm)		
		0	200	400	0	200	400
Mononuclear cell leukemia	M	28/50*	37/48*	37/50*	56.0	77.1	74.0
	F	18/49*	30/50*	29/50*	36.1	60.0	58.0
Renal tubule adenoma or carcinoma	M	1/47 <sup>(c)</sup>	3/42	4/40	2.1	7.1	10.0
Brain glioma	M	1/44 <sup>(c)</sup>	0/37	4/35	2.3	0.0	11.4
Testicular interstitial cell	M	35/49 <sup>(c)</sup>	39/46	41/50	71.4	84.8	82.0

(a) Tumor-incidence denominator adjusted by excluding animals dying before the first corresponding tumor type observed in each study.

(b) Statistical test indicators: (\*) P-value < 0.05; (\*\*) P-value < 0.005. Fisher exact test results are as reported by NTP. The control group column indicates the results of trend tests. Both the Cochran-Armitage trend test (reported by NTP) and the exact trend test calculated by OEHHA gave the same indications of significance.

(c) Although testicular tumors and brain glioma did not appear to be significantly increased by the Fisher exact and trend tests, life table tests conducted by NTP did show significant increases in trends of <0.001, and 0.039 respectively. In addition, NTP's incidental tumor tests showed increased testicular tumors by both trend and pair-wise comparisons. The life table trend test for kidney tumors was nearly significant at 0.054.

NTP (1986) conducted a study where B6C3F1 mice and F344/N rats, in groups of 50, were exposed to PCE (99.9% pure) by inhalation, 6 hours/day, 5 days/week for 103 weeks. Mice were exposed to concentrations of 100 or 200 ppm, and rats to 200 or 400 ppm, in addition to controls. The general status and body weight of the animals were monitored during the study. Upon death, animals were necropsied and histopathologic examination of all relevant tissues was performed on all animals. Approximately 70 percent or more of both sexes of mice and rats were alive at week 90 of the study. Survival was significantly reduced in male rats at the higher exposure level when compared with controls. Survival was decreased in both dose levels in male mice and in the high dose group of female mice.

As shown in Table 4, PCE significantly increased the rate of hepatocellular carcinomas in mice of both sexes. The combined incidence of liver adenoma or carcinoma was also increased, although the incidence of liver adenomas separately was not. In female and male rats, PCE also produced significant increases in mononuclear cell leukemia (MCL).

Male rats additionally exhibited apparent increases in tumor incidence in the kidney, brain, and testes. Statistical tests for increases in renal tubular-cell adenomas and adenocarcinomas appeared to be dose-related, but did not reach customary significance levels. However, the historical incidence of these tumors is low (0.4%) at the laboratory and increased incidence has been found with other chlorinated ethanes and ethylenes. Thus renal tubular-cell tumors were judged to be related to PCE exposure. Brain glioma, another rare tumor type in F344 rats, was observed in one male control rat and in four male rats at 400 ppm exposure. This increase was not statistically significant. However, because the historical incidence of these tumors is 0.8% for the laboratory, the increased brain tumor incidence in this study was also carried through the analysis. Testicular interstitial cell tumors showed significant dose-responses in both life table and incidental tumor tests calculated by NTP. This tumor type was therefore included in the dose-response evaluation, but was considered to be more uncertain, given the high background rate of testicular tumors in F344 rats (both historically and in the NTP study controls).

#### Primary Studies for the Dose-Response Assessment

Both the NTP (1986) and JISHA (1993) inhalation studies were judged to be of high quality and suitable for the development of an inhalation potency factor. The studies used different strains of mice (Crj:BDF<sub>1</sub> vs. B6C3F<sub>1</sub>) and different substrains of F344 rats. They displayed variability of outcome with respect to the tissues affected, as well as the strength of the dose-response relationships for various tumor types, and differing incidence rates in the control groups. Some of this variability could be due, in the case of the rat models, to the fact that the different substrains used may have genetic and phenotypic variation as a result of mechanisms such as genetic drift.

For example, Tiruppathi *et al.* (1990) and Thompson *et al.* (1991) reported that the Japanese and German substrains of the Fischer 344 (F344) rat, but not the US substrain, were deficient in dipeptidyl dipeptidase-4 activity in the kidney and liver. This enzyme has been implicated in the degradation of collagen, blood clotting, immunomodulation, and metabolism of hormonal peptides (Tiruppathi, *et al.*, 1990). While this particular enzymatic variation may not be directly relevant to PCE metabolism, it indicates that F344 rat substrains can display significantly divergent biological traits. With regard to the mice, the

genetic variation issue is accentuated by the use of two different mouse hybrid strains, not substrains.

Although it cannot be determined whether the different outcomes for mice and rats observed by NTP (1986) and JISHA (1993) resulted from differences in animal biology, the data suggest that each study provides non-redundant information for the analysis.

The JISHA dataset offers the advantage of an additional dose category for each species, as well as the use of several lower exposure concentrations. Moreover, the control rate of MCL incidence in the F344/DuCrj rats used in the Japanese study (22 and 20%) was significantly lower than for the F344/N rats used in the NTP study (56 and 36%), and is expected to improve the precision of the fitted model. The NTP study, nonetheless, provides important additional data on tumor development in the kidney, brain, and testes of F344/N rats, and supporting data on the dose-response rate for MCL.

Based on the above considerations, OEHHA chose both the JISHA (1993) and NTP (1986) bioassays as primary studies for the dose-response analysis. The dose-response data and results of statistical tests are presented in Tables 3 and 4. Given the availability of two acceptable inhalation studies, the oral NCI (1977) study was not used in the quantitative analysis.

#### Relevance of MCL to Humans

Some concerns about the propriety of using the rat MCL data for human risk assessment were raised by an NRC expert panel (without consensus) during a review of US EPA's PCE IRIS evaluation (NRC 2010). One issue brought up by the panel was that MCL is a common tumor in aging F344 rats that lacks a corresponding tumor in humans. Panel members also questioned the statistical significance of the MCL dose-response data in light of the elevated historical and control-group incidence rates for MCL. This section briefly addresses both questions.

Regarding the issue of tumor-site concordance, current research in cancer biology indicates that the basic cellular mechanisms of carcinogenesis are similar among mammals. However, this does not imply that exposure to a chemical carcinogen will always produce cancer in the same organ in different species (US EPA, 2005). In the case of human leukemias and lymphomas that are known to be induced by specific carcinogens, rodents develop different types of leukemia and lymphoma (US EPA, 2012c). The sites of induced cancer may not be the same because of differing toxicokinetics and tissue susceptibilities. For leukemia and lymphoma, variation in susceptibility could be related to differences in hematopoiesis and immune surveillance. Accordingly, there is no expectation—in general or specifically for MCL—of tumor-site concordance when using animal studies to predict human cancer risk (OEHHA, 2009).

Notwithstanding this general principle, there is evidence that rat MCL corresponds to at least one form of human leukemia. The specific cell type and biological mechanisms that give rise to rat MCL are not known, but it appears to arise from a lymphocyte or monocyte lineage, and it is thought that the cell of origin resides in the spleen or undergoes neoplastic transformation in the spleen (Thomas *et al.*, 2007). One reasonable hypothesis is that rat MCL is a form of Large Granular Lymphocyte Leukemia (LGLL), a cancer that

develops in the spleen and is phenotypically and functionally similar to human LGLL (IARC, 1990; Thomas *et al.*, 2007). Human LGLL derives from either T-cell or natural killer (NK) cell lineages (Sokol and Loughran, 2006). Additional support for linking rat MCL to human LGLL is provided by a study using the F344 rat MCL as a model for human NK-LGLL, which observed similar cellular responses in samples of the two tumor-cell types (Liao *et al.*, 2011).

Exposure of humans and animals to relatively low doses of PCE produces adverse effects upon blood and the immune system (e.g., see: Marth, 1987; Kroneld, 1987; and Emara *et al.*, 2010) that could plausibly give rise to a variety of carcinogenic response in different species. In addition to human LGLL, rat MCL may correspond to other types of human leukemia or lymphoma.

Regarding statistical issues arising from the elevated incidence of MCL in control groups, an NTP workshop focusing on the high background incidences of MCL and other tumors in the F344 rat noted that, "From a statistical perspective, high background rates of such tumors in control animals will generally decrease the ability to detect an exposure-related effect. In addition, when a statistically significant tumor effect is found in test animals relative to concurrent controls, the effect may not be considered exposure-related if it falls within the range observed in historical controls" (King-Herbert and Thayer, 2006). The foregoing statement focuses on the problem of false negative test results. However, since US EPA found MCL incidence to be significantly elevated in PCE-exposed rats, NRC panel members were concerned with the potential for false positive test results. On this issue, OEHHA agrees with the Massachusetts Department of Environmental Protection (MDEP), who reviewed the historical background rates of MCL in the NTP and JISHA study laboratories and found that,

"For both the NTP (1986) and JISHA (1993) studies, the background rate of MCL in the same study control group was greater than or equivalent to the historical control rates for the same lab, same sex. Thus, the controls in both studies did not exhibit anomalously low MCL, which could, had it occurred, lead to false positive responses in the treatment groups." (MDEP, 2014)

Indeed, for the JISHA male rat MCL data, where the incidence in study controls was 22%, the historical incidence was 6-22%, and the Cochran-Armitage test for trend was highly significant, having a p-value of less than 0.0005.

## 8. MODE(S) OF ACTION

PCE's carcinogenic modes of action (MOA) likely involve the genotoxicity of one or more of its oxidative- or GST-pathway metabolites, although the precise mechanisms are unknown.

Several PCE metabolites, e.g., PCE epoxide, oxalyl chloride, trichloroacetyl chloride, dichlorothioketene, and the TCVC sulfoxides, are reactive compounds and expected to have short half-lives in the nucleophile-rich cellular environment.<sup>8</sup> These substances will

---

<sup>8</sup> For example, the high reactivity of PCE epoxide is indicated by its 2.6-minute half-life in a neutral aqueous buffer solution at 37 °C (Yoshioka, *et al.*, 2002).

tend to react chemically and enzymatically with cellular components near their site of production. The relatively stable metabolites, such as: TCA, DCA, TCVC, and N-AcTCVC, are more likely to circulate throughout the body where they may be further metabolized and impact tissues other than the liver and kidney.

Both trichloroacetic acid (TCA) and dichloroacetic acid (DCA) have independently been found to increase tumor formation in mice. Since TCA is a major metabolite of PCE, US EPA (2012a) evaluated whether it could be the primary source of PCE's carcinogenicity in mouse liver. Using dose-response data from the JISHA (1993) and NTP (1986) PCE studies and a drinking water study of TCA in mice (DeAngelo, *et al.*, 2008), US EPA found that metabolically-generated TCA could contribute from 12 to 100 percent of the increased risk of liver tumors. This large range is not highly informative, and leaves open the possibility that other reactive metabolites may contribute significantly to the production of liver tumors in mice.

There are several non-genotoxic MOAs that may contribute to PCE's carcinogenicity, though in as yet poorly understood ways. These have been discussed at length by US EPA (2012a), and include: cytotoxicity with subsequent cellular proliferation, oxidative stress-induced cellular transformation, and dysregulation due to altered DNA methylation. Two specific MOAs that are potentially relevant for evaluating PCE involve  $\alpha$ 2u-globulin nephropathy in the male rat, and PPAR $\alpha$  activation<sup>9</sup> for mouse liver tumors. In both cases, the biological bases for these MOAs in rodents are thought to be muted or absent in humans, indicating that the particular tumor-types may not be useful for human risk assessment.

#### *$\alpha$ 2u-Globulin Nephropathy*

The  $\alpha$ 2u-globulin MOA in male rats is defined by: accumulation of  $\alpha$ 2u-globulin-containing hyaline droplets in the proximal tubules of the kidney, cytotoxicity with tubular cell proliferation, exfoliation of epithelial cells into the proximal tubular lumen and formation of granular casts, papillary mineralization, hyperplastic foci, and renal tumors (US EPA, 1991).

Green *et al.* (1990) found accumulation of  $\alpha$ 2u-globulin in the proximal tubules of F344 rats exposed by inhalation to 1000 ppm of PCE for 10 days, or given 1500 mg/kg PCE by gavage for 42 days. However a 400 ppm inhalation exposure for 28 days did not produce protein droplets or other signs of toxicity. For chemicals known to cause  $\alpha$ 2u-globulin toxicity, the formation of protein droplets in the kidney occurs rapidly upon exposure (frequently after a single dose), and further indications of tissue damage begin to appear in 3 to 4 weeks (Lehman-McKeeman, 2010; Green *et al.*, 1990). Thus, the absence of  $\alpha$ 2u-globulin accumulation after a 28-day exposure suggests that 400 ppm of PCE will not result in  $\alpha$ 2u-globulin toxicity upon long-term exposures.

The NTP (1986) study provided additional evidence along these lines. Karyomegaly and cytomegaly were observed in the kidneys of rats exposed to 200 or 400 ppm for 2 years, but indicators of  $\alpha$ 2u-globulin nephropathy (e.g., hyaline droplets, mineralization, and cast formation) were not found. The NTP protocol at the time was not designed to detect

---

<sup>9</sup> PPAR $\alpha$  = "peroxisome proliferator-activated receptor- $\alpha$ ."

hyaline droplets or  $\alpha$ 2u-globulin accumulation (US EPA 2012a) but would have observed other markers of  $\alpha$ 2u-globulin toxicity if this MOA had been in effect. Moreover, comparable toxicity was observed in female rats in the NTP study, and PCE caused similar kidney damage in rats and mice of both sexes in the NCI (1977) gavage study. This suggests that PCE's nephrotoxicity is neither sex nor species specific, as would be expected with an  $\alpha$ 2u-globulin MOA.

### PPAR $\alpha$ Activation

The PPAR $\alpha$  MOA involves activation of the PPAR $\alpha$  nuclear receptor, which is hypothesized to cause alterations in cell proliferation and apoptosis, and clonal expansion of initiated cells. The proposed indicators for this mode of action are: (1) PPAR $\alpha$  activation with associated peroxisome proliferation, or (2) PPAR $\alpha$ -activation plus increased liver weight and effects such as increased peroxisomal  $\beta$ -oxidation, CYP4A, or acyl CoA oxidase (Klaunig, *et al.*, 2003).

Numerous studies have been carried out to verify the PPAR $\alpha$  MOA. The evidence obtained from this body of research has been mixed, and it currently remains unclear whether this hypothetical MOA is a major causal factor in mouse-liver tumor formation. The US EPA has published several detailed reviews of the PPAR $\alpha$  MOA in its IRIS program toxicity reviews for PCE and TCA (US EPA 2012a, 2011). The main conclusions of these reviews are:

- PPAR $\alpha$  activators can produce multiple effects in addition to peroxisome proliferation, including genotoxicity, oxidative stress, hypomethylation of DNA, and activation of other nuclear receptors.
- Peroxisome proliferation and the associated markers of PPAR $\alpha$  activation are poor predictors of hepatocarcinogenesis in mice and rats. Studies with various PPAR $\alpha$  activators show that the correlation between *in vitro* PPAR $\alpha$  activation potency and tumorigenesis is weak and this relationship does not appear to be due to differences in pharmacokinetics. This suggests the involvement of carcinogenic mechanisms other than PPAR $\alpha$ -activation.
- Studies of the PPAR $\alpha$ -agonist, diethyl hexyl phthalate (DEHP) in transgenic mouse strains, although not fully conclusive, have cast doubt on whether the key events in the PPAR $\alpha$  MOA (receptor activation, hepatocellular proliferation, and clonal expansion) are sufficient to cause liver tumors. The studies suggest that DEHP can induce tumors in a PPAR $\alpha$ -independent manner (Ito *et al.*, 2007a), and that PPAR $\alpha$  activation in hepatocytes is insufficient to cause tumorigenesis (Yang *et al.*, 2007). This again indicates that other mechanisms, either independently or in combination with PPAR $\alpha$ -activation, are necessary to induce tumors.

- PCE exposure leads to PPAR $\alpha$ -activation and modest levels of peroxisome proliferation, predominantly through its metabolite TCA. There is conflicting evidence as to whether this causes cellular proliferation in animals exposed to PCE: the peroxisome proliferation caused by PCE lacks specificity and consistency with respect to tissue, species, dose, and sequence of events. Also, there is little evidence indicating that PCE can induce clonal expansion of initiated cells. The available information for PCE is insufficient to demonstrate that the PPAR $\alpha$  MOA plays a significant causative role in mouse hepatocarcinogenesis.

#### Conclusion on PCE's Mode(s) of Action

Given the limited understanding of the various non-genotoxic MOAs that may modify or add to the tumorigenic effects of PCE's genotoxic metabolites, there are insufficient grounds to evaluate PCE as primarily a non-genotoxic carcinogen using a non-linear model.

### 9. DOSE-RESPONSE ASSESSMENT

#### Dose Metrics

Much of the following information has already been presented, but is briefly restated here because of its relevance to choosing metrics for the dose-response calculations:

- The liver is the main site of oxidative PCE-metabolite formation, but other tissues with CYP 450 2E1, 2B, and 3A activity may also contribute to the oxidative-pathway. TCA is a relatively stable metabolite that has been found to increase liver tumors in mice via oral exposure. TCA's cancer potency in other tissues has not been adequately examined.
- Of the two metabolic pathways, oxidation is the main pathway in rodents. For example, at 10 ppm exposure, the PBPK model indicates that the ratio of oxidation to glutathione conjugation is 600 in mice and 19.5 in rats.
- Saturation of the oxidative pathway begins to occur between 1 and 10 ppm exposure in mice, and between 10 and 100 ppm exposure in rats (see Table 1). Saturation causes the ratio of oxidized to absorbed PCE to decrease at higher exposure concentrations. The smaller amount of metabolism that occurs via the GST pathway, on the contrary, increases somewhat at higher exposure concentrations in rodents.
- Although most GST conjugation of PCE takes place in the liver, the kidney is likely to be the main site for production of reactive GST-pathway metabolite dichlorothioketene. Other metabolites such as: TCVC, N-AcTCVC, and TCVC sulfoxide are formed in both the liver and kidney, and may circulate to other metabolizing tissues as well.
- It is not known which PCE metabolites, or even which of the two main metabolic pathways produces the most carcinogenic risk.
- The PBPK model for the GST pathway in humans involves a large variability or uncertainty, with two possible values (posterior modes) for the rate of PCE conjugation that differ by a factor of approximately 3000. However, as was

discussed earlier in Section 6, the impact of the human PBPK model uncertainty/variability upon the overall dose-response evaluation is several orders of magnitude lower than this. It is not known how much of the model variability is due to the wide range of GST activities that have been observed in the human population, but it is reasonable to assume that some segment of the population could be efficient metabolizers while other segments (e.g., individuals who are homozygous in GST-null variants) could be much less efficient. It is currently unclear which GST isoforms are most active with regard to PCE conjugation.

- The more probable and larger of the two values indicates that glutathione conjugation predominates over oxidation in humans, the ratio of PCE conjugation to oxidation being about 10.

OEHHA considered the advantages and disadvantages of using several dose metrics for the dose-response calculations. These are briefly discussed below.

- Applied air concentration: This would be the simplest approach in that it does not rely upon the output of complicated PBPK modeling calculations. However, given the large body of evidence indicating that PCE's metabolites are likely to be responsible for its tumorigenic properties, using applied concentration as the dose metric may reduce the accuracy of the dose-response analysis, especially for the mouse, where the dose-response data indicate significant metabolic saturation in the oxidative pathway at the higher PCE exposure concentrations tested.
- PCE blood concentration: This dose metric does make use of the PBPK modeling estimates but has the same weakness as using the applied air concentration, since blood concentrations of the parent compound may not be directly related to concentrations of the potentially carcinogenic metabolites of PCE. Blood concentrations of PCE may even be less accurate than applied concentrations, since PCE blood concentrations are expected to be inversely related to metabolite concentrations (For example, see Table 1 entries for the mouse dose-metrics where "PCE AUC per ppm exposure" increases and "percent oxidation/ppm" decreases) as one moves to higher exposure concentrations).
- Pathway specific metabolized dose: Defining a dose metric based upon either the oxidation or GST conjugation pathway would be better in terms of focusing on the production of PCE's carcinogenic metabolites instead of the parent compound. However, using either of the two pathways alone would be problematic, since each pathway produces several genotoxic substances that could be important for PCE's overall tumorigenicity. From Table 1 it can be seen that for mice, the quantity of oxidative metabolites produced with increasing exposure appears to be inversely related to the quantity of conjugation metabolites. Furthermore, if humans are more efficient conjugators than rodents, using an oxidation-only dose metric could underestimate the dose-response function. On the other hand, using glutathione conjugation alone has the problem of large model uncertainties with larger impacts upon the overall dose-response assessment (note that this impact is muted for total metabolism, as discussed above in Section 6).

- Choosing one or more metabolites: Using a subset of concentrations of one or more metabolites for the dose metric has similar problems as using pathway specific metabolism. For example, in Section 8 we briefly discussed US EPA's evaluation of TCA, a major metabolite generated in the oxidation pathway, where it was estimated that TCA might be responsible for as little as 12 percent of liver tumor risk in mice. An added issue is that the available PBPK models only incorporate a few of the various metabolites, such as TCA and DCA.
- Total PCE metabolized dose: Using total metabolism for the dose metric accounts for toxicokinetic differences across species and provides a dose adjustment for saturation effects in the oxidative pathway. It has the advantage of taking into account both pathways generating potentially carcinogenic metabolites. However, it involves assuming that carcinogenic potency is proportional to the combined rate of the first step of metabolism in each pathway. This assumption is simplistic but unavoidable given the many unknowns involved in PCE's toxicokinetics and toxicodynamics. As noted above, total metabolized dose has an advantage over using either oxidative or glutathione conjugation alone. Using oxidation-only may not be adequately protective of human health given the potential genotoxicity of metabolites formed in the conjugation pathway. Total metabolized dose is also advantageous compared with using the GST-pathway metabolites alone, since the PBPK modeling uncertainties have relatively little impact upon the dose-response assessment using total metabolism as the metric.

Considering all of the above factors, total metabolism was chosen as the best dose metric for the dose-response analysis of all the tumor types identified in the primary mouse and rat studies.<sup>10</sup> The PBPK-estimated, total metabolized doses used in the dose-response analysis are presented in Appendix B.

#### Dose-Response Model

Based upon its metabolic profile and the genotoxic activity of some of the metabolites formed, OEHHA considers PCE to be a genotoxic carcinogen. This information supports the assumption that the dose-response relationship approaches linearity at low doses and the use of the multistage cancer model to estimate the potency factor. This is consistent with OEHHA risk assessment guidelines, which indicate that use of the multistage model (and assuming low-dose linearity) is reasonable under such circumstances (OEHHA, 2009). In the traditional, linearized-multistage model, cancer potency is estimated as the upper 95% confidence bound, ( $q_1^*$ ), on the linear coefficient ( $q_1$ ) in the following expression relating lifetime probability of cancer ( $p$ ) to dose ( $d$ ):

$$p = q_0 + (1 - q_0)(1 - \exp[-(q_1d + q_2d^2 + \dots)])$$

In the above equation, ( $d$ ) represents the average daily dose resulting from a uniform, continuous exposure over the nominal lifetime of the animal (two years for both mice and

<sup>10</sup> [In using total metabolized dose as the preferred dose metric, OEHHA considered the uncertainty in the available scientific information and, in contrast to US EPA \(2012a\), has chosen a modeling approach that will produce a more health-protective potency estimate. This is consistent with the OEHHA's cancer risk assessment guidelines \(OEHHA 2009\), which establish a policy of developing cancer potency factors that are adequate to protect public health.](#)

rats); ( $q_0$ ) is the tumor incidence in the non-exposed group. For studies where the exposures vary in time, they are averaged over the entire study period and modeled as if they were uniform and continuous. Prior to fitting the dose-response model to the study data, an adjustment is made to the incidence rates to account for inter-current mortality, which decreases the pool of animals at risk of developing tumors throughout the study.

The latest version of BMDS (Version 2.6.0.1, US EPA, 2015) was used to carry out the necessary dose-response calculations. The BMDS dichotomous multi-stage cancer model was run for all allowed degrees of the approximating polynomial, with a benchmark risk (BMR) of 5 percent. Instead of ( $q_1^*$ ) the software calculates benchmark doses (BMDs) and their 95% lower confidence levels (BMDLs). When multiplied by the BMR, the reciprocal of the BMDL gives a unit risk factor that is generally close in value to, and is used in place of ( $q_1^*$ ). For each tumor site, the model with the lowest value of AIC (Akaike's Information Criterion) was chosen, as long as its p-value for goodness-of-fit was above 0.1 and the absolute value of the scaled residual for the dose near the BMD was less than 2.0. The optimal model typically resulted from fitting a polynomial of 1 or 2 degrees, and the models with the lowest AIC also had the highest p-values (signifying the best fit to the data).

Interspecies extrapolation from experimental animals to humans was based on body weights ( $bw$ ) raised to three-quarters power (US EPA, 2005; Anderson *et al.*, 1983), which for BMDLs, may be expressed in terms of body weight raised to one-quarter power, as follows:

$$BMDL_{(Human)} = BMDL_{(Animal)} \times \left( \frac{bw_{(Animal)}}{bw_{(Human)}} \right)^{1/4}$$

The above equation is presumed to account for the toxicokinetic and toxicodynamic differences between species. Toxicokinetic modeling can sometimes eliminate the need for toxicokinetic scaling between animals and humans. This would be the case, for example, if the dose metric used in the analysis was the AUC of a directly carcinogenic metabolite. The remaining toxicodynamic differences would then be addressed, according to OEHHA practice, by scaling according to the one-eighth power of the body weight ratio.<sup>11</sup> Using the rate of PCE metabolism as a dose metric, on the other hand, does not account for the toxicokinetics of other downstream biological processes that determine tissue concentrations of the relevant carcinogenic species. In this case, the full cross-species scaling factor is used (US EPA, 1992).

Since PCE induced tumors at multiple sites in male mice (JISHA study) and male rats (NTP study), the combined cancer potency was also estimated for these groups using the multi-site tumor module provided in BMDS. The BMDS procedure for summing risks over several tumor sites uses the profile likelihood method. In this method, the maximum likelihood estimates (MLEs) for the multistage model parameters ( $q_i$ ) for each tumor type are added together (*i. e.*,  $\sum q_0, \sum q_1, \sum q_2$ ), and the resulting model is used to determine a combined BMD. Then a confidence interval for the combined BMD is calculated by computing the desired percentile of the chi-squared distribution associated with a likelihood ratio test having one degree of freedom.

---

<sup>11</sup> US EPA risk assessment guidelines (2005) suggest "retaining some of the cross-species scaling factor (e.g., using the square root of the cross-species scaling factor)," when toxicokinetic modeling is used without toxicodynamic modeling.

Once the organ-specific and multi-site BMDLs were obtained and scaled by body-weight, the toxicokinetic model was used to estimate the continuous 24-hour air concentration that would produce the same daily metabolized dose for an adult human (i.e., the human equivalent concentration or "HEC"). The cancer potency values were then calculated by dividing the BMR of 0.05 by the HEC. Table 5 provides the calculated BMDs, BMDLs, and the interspecies-adjusted BMDLs for individual and combined tumor sites. Potency values derived from the primary studies are presented in Table 6 as unit risks factors (URFs) with units of reciprocal  $\mu\text{g}/\text{m}^3$ .

#### Inhalation Potency Value for PCE

The updated carcinogenic potency value for PCE is based on the following observations and rationale:

- Tissue-specific URF values calculated from the JISHA study are of similar magnitude to the corresponding URFs obtained from the NTP study, though somewhat lower. For mouse liver tumors, the ratio of the JISHA UR to the NTP UR was about 0.8 in both females and males. For rat MCL the corresponding ratios were 0.4 for females and 0.6 for males. The smaller URF values from the JISHA data may be due in part to the higher precision obtained by the study having used lower doses and an additional dose group.
- In both studies, the males of both species appeared to be more sensitive than the corresponding females to the tumorigenic effects of PCE.
- The URF values from both studies ranged from 2.8E-06 to 1.6E-05 (per  $\mu\text{g}/\text{m}^3$ ), within a factor of 6. (The compared values included the multi-tumor risks for male NTP rats and male JISHA mice, as well as tissue-specific risks for other organs in mice and rats of both sexes.) Looking only at males of each species, the URFs ranges from 4.0E-06 to 1.6E-05.
- The highest URF was obtained from the combined site (i.e., multi-tumor) risk in male rats in the NTP study. This value was obtained by including MCL, brain, testicular, and renal tumors in the multi-tumor calculation.
- The URF values for mouse liver tumors and rat MCL were judged by OEHHA to be more certain in view of the qualitative and quantitative agreement between the two primary studies; mouse liver tumors were also found in the NCI (1977) oral exposure study.
- The unique tumors seen in the NTP study, including kidney tumors, are important to consider. The kidney is one site where the GST-pathway may contribute substantially to the cancer potency. Moreover, there is reasonable evidence that the GST-pathway may also contribute to tumorigenesis in other organ systems.
- Although it appears likely that PCE exposure increased the rate of testicular tumors in rats, the relatively high risk value obtained for testicular tumors in NTP rats may be more uncertain, given the high tumor incidence seen in the control group (71%).

Considering the above points, and also that the set of calculated values is clustered in a narrow range, the geometric mean of the male mouse and rat URFs from both studies

was chosen as the best estimate of PCE cancer potency. Specifically, the geometric mean was calculated using the URF values shown in Table 7. The resulting URF, when rounded to two significant figures, is  $6.1\text{E-}06$  ( $\mu\text{g}/\text{m}^3$ )-1. A cancer slope factor of  $2.1\text{E-}02$  (per mg/kg-day) was also calculated from the URF using an adult body weight of 70 kg and an inspiration rate of 20 m<sup>3</sup>/day.

<b>Table 5: BMD5 Modeling Results for the Primary Studies</b>								
<b>Study</b>	<b>Sex</b>	<b>Tumor Type</b>	<b>P-value for multi-stage model fit</b>	<b>Scaled residual for dose near the BMD</b>	<b>BMD (mg/kg-day)</b>	<b>BMDL (mg/kg-day)</b>	<b>Animal BW (kg)</b>	<b>BW-Scaled BMDL (mg/kg-day)</b>
<b>Results from Mouse Studies</b>								
JISHA	M	Hepatocellular adenoma or carcinoma	0.22	1.17	3.06	2.16	0.048	0.350
		Harderian gland	0.99	-0.06	38.56	12.34	0.048	1.997
		Hemangioma or Hemangiosarcoma	0.35	0.94	26.61	12.98	0.048	2.100
		Combined site			2.73	1.85	0.048	0.300
	F	Hepatocellular adenoma or carcinoma	0.77	-0.23	10.33	3.84	0.035	0.574
NTP	M	Hepatocellular adenoma or carcinoma	0.85	0.03	2.46	1.79	0.037	0.272
	F	Hepatocellular adenoma or carcinoma	0.82	0.05	11.27	3.15	0.025	0.432
<b>Results from Rat Studies</b>								
JISHA	M	Mononuclear cell leukemia	0.79	0.07	1.34	0.89	0.45	0.251
	F	Mononuclear cell leukemia	0.37	1.05	3.99	1.84	0.30	0.472
NTP	M	Mononuclear cell leukemia	0.23	-0.31	0.92	0.51	0.44	0.144
		Testicular interstitial cell	0.35	-0.26	1.06	0.48	0.44	0.136
		Renal adenoma or carcinoma	0.93	0.07	6.76	3.24	0.44	0.913
		Brain glioma	0.15	0.62	9.45	5.07	0.44	1.426
		Combined site			0.46	0.28	0.44	0.078
	F	Mononuclear cell leukemia	0.25	-0.30	1.24	0.72	0.32	0.188

<b>Table 6: Unit Risk Factors from Primary Studies</b>					
<b>Study</b>	<b>Sex</b>	<b>Tumor Type</b>	<b>BW-Scaled BMDL (mg/kg-day)</b>	<b>HEC based on PBPK Model (ppm)</b>	<b>Unit Risk Factor (URF) per <math>\mu\text{g}/\text{m}^3</math></b>
<b>Results from Mouse Studies</b>					
JISHA	M	Hepatocellular adenoma or carcinoma	0.350	2.14	3.5E-06
		Harderian gland	1.997	12.20	6.0E-07
		Hemangioma or Hemangiosarcoma	2.100	12.83	5.7E-07
		Combined site	0.300	1.83	4.0E-06
	F	Hepatocellular adenoma or carcinoma	0.574	3.51	2.1E-06
NTP	M	Hepatocellular adenoma or carcinoma	0.272	1.66	4.4E-06
	F	Hepatocellular adenoma or carcinoma	0.432	2.64	2.8E-06
<b>Results from Rat Studies</b>					
JISHA	M	Mononuclear cell leukemia	0.251	1.53	4.8E-06
	F	Mononuclear cell leukemia	0.472	2.88	2.6E-06
NTP	M	Mononuclear cell leukemia	0.144	0.88	8.4E-06
		Testicular interstitial cell	0.136	0.83	8.9E-06
		Renal adenoma or carcinoma	0.913	5.57	1.3E-06
		Brain glioma	1.426	8.71	8.5E-07
		Combined site	0.078	0.47	1.6E-05
	F	Mononuclear cell leukemia	0.188	1.15	6.4E-06

<b>Table 7: URFs Used to Calculate Mean</b>		
<b>Species</b>	<b>Study</b>	<b>URF (<math>\mu\text{g}/\text{m}^3</math>)<sup>-1</sup></b>
Male Mouse	JISHA (Multiple tumor)	4.02E-06
	NTP (Liver)	4.44E-06
Male Rat	JISHA (MCL)	4.81E-06
	NTP (Multiple tumor)	1.57E-05
	Geometric Mean	6.06E-06

## 10. REFERENCES

- Anders MW, Lash L, Dekant W, Elfarra AA, Dohn DR, Reed DJ. 1988. Biosynthesis and biotransformation of glutathioneS-conjugates to toxic metabolites. *CRC Critical Reviews in Toxicology* 18:311-341.
- Anderson EL. 1983. Quantitative Approaches in Use to Assess Cancer Risk. *Risk Analysis* 3:277-295.
- ARB. 2012. California Environmental Protection Agency, Air Resources Board, Air Toxic Emissions Inventory, 2012.
- Birner G, Richling C, Henschler D, Anders MW, Dekant W. 1994. Metabolism of tetrachloroethene in rats: identification of N epsilon-(dichloroacetyl)-L-lysine and N epsilon-(trichloroacetyl)-L-lysine as protein adducts. *Chemical Research in Toxicology* 7:724-732.
- Birner G, Rutkowska A, Dekant W. 1996. N-acetyl-S-(1,2,2-trichlorovinyl)-L-cysteine and 2,2,2-trichloroethanol: Two novel metabolites of tetrachloroethene in humans after occupational exposure. *Drug Metabolism and Disposition* 24:41-48.
- Bull RJ, Sasser LB, Lei XC. 2004. Interactions in the tumor-promoting activity of carbon tetrachloride, trichloroacetate, and dichloroacetate in the liver of male B6C3F<sub>1</sub> mice. *Toxicology* 199:169-183.
- CDHS. 1991. California Department of Health Services. Health Effects of Tetrachloroethylene (PCE). Berkeley, CA.
- Chiu WA, Ginsberg GL. 2011. Development and evaluation of a harmonized physiologically based pharmacokinetic (PBPK) model for perchloroethylene toxicokinetics in mice, rats, and humans. *Toxicology and Applied Pharmacology* 253:203-234.
- Clewell HJ, Gentry PR, Kester JE, Andersen ME. 2005. Evaluation of physiologically based pharmacokinetic models in risk assessment: an example with perchloroethylene. *Critical Reviews in Toxicology* 35:413-433.
- Dallas CE, Chen XM, O'Barr K, Muralidhara S, Varkonyi P, Bruckner JV. 1994. Development of a physiologically based pharmacokinetic model for perchloroethylene using tissue concentration-time data. *Toxicology and Applied Pharmacology* 128:50-59.
- DeAngelo A B, Daniel FB, Wong DM, George MH. 2008. The induction of hepatocellular neoplasia by trichloroacetic acid administered in the drinking water of the male B6C3F<sub>1</sub> mouse. *Journal of Toxicology and Environmental Health A71*:1056-1068.
- Dekant W. 1986. Metabolic conversion of tri- and tetrachloroethylene: formation and deactivation of genotoxic intermediates. *Developments in Toxicology & Environmental Science* 12:211-221.
- Dekant W, Birner G, Werner M, Parker J, 1998. Glutathione conjugation of perchloroethene in subcellular fractions from rodent and human liver and kidney. *Chemico-Biological Interactions* 116: 31-43.

Dekant W, Martens G, Vamvakas S, Metzler M, Henschler D. 1987. Bioactivation of tetrachloroethylene: role of glutathione S-transferase-catalyzed conjugation versus cCytochrome P-450-dependent phospholipid alkylation. *Drug Metabolism and Disposition* 15:702-709.

Dekant W, Metzler M, Henschler D. 1986. Identification of S-1,2,2-trichlorovinyl-N-acetylcysteine as a urinary metabolite of tetrachloroethylene: bioactivation through glutathione conjugation as a possible explanation of its nephrocarcinogenicity. *Journal of Biochemical Toxicology* 1:57-72.

DeMarini DM, Perry E, Shelton ML. 1994. Dichloroacetic acid and related compounds: induction of prophage in *E. coli* and mutagenicity and mutation spectra in *Salmonella* TA100. *Mutagenesis* 9:429-437.

Dow. 2008. The Dow Chemical Company. Product Safety Assessment, Perchloroethylene. June 24, 2008.

Emara AM, Abo El-Noor MM, Hassan NA, Wagih AA. 2010. Immunotoxicity and hematotoxicity induced by tetrachloroethylene in Egyptian dry cleaning workers. *Inhalation Toxicology* 22:117-124.

Fernandez J, Guberan E, Caperos J. 1976. Experimental human exposures to tetrachloroethylene vapor and elimination in breath after inhalation. *American Industrial Hygiene Association Journal* 37:143-150.

Frantz SW, Watanabe PG. 1983. Tetrachloroethylene: balance and tissue distribution in male Sprague-Dawley rats by drinking-water administration. *Toxicology and Applied Pharmacology* 69:66-72.

Green T, Odum J, Nash JA, Foster JR. 1990. Perchloroethylene-induced rat kidney tumors: an investigation of the mechanisms involved and their relevance to humans. *Toxicology and Applied Pharmacology* 103:77-89.

Guyton KZ, Chiu WA, Bateson TF, Jinot J, Scott CS, Brown RC, Caldwell JC. 2009. A reexamination of the PPAR-alpha activation mode of action as a basis for assessing human cancer risks of environmental contaminants. *Environmental Health Perspectives* 117:1664-1672.

Guyton KZ, Hogan KA, Scott CS, Cooper GS, Bale AS, Kopylev L, Barone S Jr, Makris SL, Glenn B, Subramaniam RP, Gwinn MR, Dzubow RC, Chiu WA. 2014. Human health effects of tetrachloroethylene: key findings and scientific issues. *Environmental Health Perspectives* 122:325-334.

Hannon-Fletcher MP, Barnett YA. 2008. Lymphocyte cytochrome P450 expression: inducibility studies in male Wistar rats. *British Journal of Biomedical Science* 65:1-6.

Hinchman CA, Ballatori N. 1994. Glutathione conjugation and conversion to mercapturic acids can occur as an intrahepatic process. *Journal of Toxicology and Environmental Health* 41:387-409.

HSDB. 2010. Hazardous Substance Data Bank. National Library of Medicine, Bethesda MD. (Internet version accessed in 2015).

IARC. 1990. International Agency for Research on Cancer. Pathology of Tumors in Laboratory Animals, 1: Tumours of the Rat. IARC Scientific Publication, No. 99, 2nd edition, Lyon France.

IARC. 2014. International Agency for Research on Cancer. Trichloroethylene, tetrachloroethylene, and some other chlorinated agents / IARC Working Group on the Evaluation of Carcinogenic Risks to Humans (2012: Lyon, France). IARC monographs on the evaluation of carcinogenic risks to humans. Vol 106.

Ikeda M, Koizumi A, Watanabe T, Endo A, Sato K. 1980. Cytogenetic and cytokinetic investigations on lymphocytes from workers occupationally exposed to tetrachloroethylene. *Toxicology Letters* 5: 251-256.

Irving RM, Elfarra AA. 2012. Role of reactive metabolites in the circulation in extrahepatic toxicity. *Expert Opinion on Drug Metabolism & Toxicology* 8:1157-1172.

Irving RM, Elfarra AA. 2013. Mutagenicity of the cysteine S-conjugate sulfoxides of trichloroethylene and tetrachloroethylene in the Ames test. *Toxicology* 306:157-161.

Ito Y, Yamanoshita O, Asaeda N, Tagawa Y, Lee CH, Aoyama T, Ichihara G, Furuhashi K, Kamijima M, Gonzalez FJ, Nakajima T. 2007. Di(2-ethylhexyl)phthalate induces hepatic tumorigenesis through a peroxisome proliferator-activated receptor alpha-independent pathway. *Journal of Occupational Health* 49:172-182.

JISHA. 1993. Japan Industrial Safety and Health Association, Japan Bioassay Research Center. Carcinogenicity study of tetrachloroethylene by inhalation in rats and mice. 2445 Hirasawa, Hadano, Kanagawa, 257-0015, Japan. March .31, 1993.

Kim S, Kim D, Pollack GM, Collins LB, Rusyn I. 2009. Pharmacokinetic analysis of trichloroethylene metabolism in male B6C3F<sub>1</sub> mice: Formation and disposition of trichloroacetic acid, dichloroacetic acid, S-(1,2-dichlorovinyl)glutathione and S-(1,2-dichlorovinyl)-L-cysteine. *Toxicology and Applied Pharmacology* 238:90-9.

King-Herbert, Thayer. 2006. NTP workshop: Animal model for the NTP rodent cancer bioassay: strain and stock - should we switch? *Toxicologic Pathology* 34: 802-805.

Klaunig JE, Babich MA, Baetcke KP, Cook JC, Corton JC, David RM, DeLuca JG, Lai DY, McKee RH, Peters JM, Roberts RA, Fenner-Crisp PA. 2003. PPAR-alpha agonist-induced rodent tumors: Modes of action and human relevance. *Critical Reviews in Toxicology* 33:655-780.

Kline SA, McCoy EC, Rosenkranz HS, Van Duuren BL. 1982. Mutagenicity of chloroalkene epoxides in bacterial systems. *Mutation Research* 101:115-125.

Kroneld R. 1987. Effect of volatile halocarbons on lymphocytes and cells of the urinary tract. *Bulletin of Environmental Contamination and Toxicology* 38:856-861.

Lash LH, Lipscomb JC, Putt DA, Parker JC. 1999. Glutathione conjugation of trichloroethylene in human liver and kidney: kinetics and individual variation. *Drug Metabolism and Disposition* 27:351-359.

Lash LH, Parker JC. 2001. Hepatic and renal toxicities associated with perchloroethylene. *Pharmacological Reviews* 53:177-208.

Lash LH, Putt DA, Parker JC. 2006. Metabolism and Tissue Distribution of Orally Administered Trichloroethylene in Male and Female Rats: Identification of Glutathione- and Cytochrome P450-Derived Metabolites in Liver, Kidney, Blood and Urine. *Journal of Toxicology and Environmental Health Part A* 69:1285-1309.

Lash LH, Putt DA, Huang P, Hueni SE, Parker JC. 2007. Modulation of hepatic and renal metabolism and toxicity of trichloroethylene and perchloroethylene by alterations in status of cytochrome P450 and glutathione. *Toxicology* 235:11-26.

Lash LH, Qian W, Putt DA, Desai K, Elfarra AA, Sicuri AR, Parker JC. 1998. Glutathione conjugation of perchloroethylene in rats and mice in vitro: sex-, species-, and tissue-dependent differences. *Toxicology and Applied Pharmacology*. 150:49-57.

Lehman-McKeeman, LD. 2010. 2u-Globulin Nephropathy, in McQueen, C. A., *Comprehensive toxicology*. 2nd ed. / Oxford: Elsevier, 2010.

Liao A, Broeg K, Fox T, Tan SF, Watters R, Shah MV, Zhang LQ, Li Y, Ryland L, Yang J, Aliaga C, Dewey A, Rogers A, Loughran K, Hirsch L, Jarbadan NR, Baab KT, Liao J, Wang HG, Kester M, Desai D, Amin S, *et al.* 2011. Therapeutic efficacy of FTY720 in a rat model of NK-cell leukemia. *Blood* 118:2793-2800.

Marth E. 1987. Metabolic changes following oral exposure to tetrachloroethylene in subtoxic concentrations. *Archives of Toxicology* 60:293-299.

Mazzullo M, Grilli S, Lattanzi G, Prodi G, Turina MP, Colacci A. 1987. Evidence of DNA binding activity of perchloroethylene. *Research Communications in Chemical Pathology & Pharmacology* 58:215-235.

MDEP. 2014. Massachusetts Department of Environmental Protection, Office of Research and Standards, Tetrachloroethylene (Perchloroethylene), Inhalation Unit Risk Value, June 25, 2014.

NCI. 1977. National Cancer Institute. Bioassay of tetrachloroethylene for possible carcinogenicity. Bethesda, Md: National Institutes of Health. Report no. NCI-CGTR-13; DHEW Publication No. (NIH) 77-813.

NRC. 2010. National Research Council. Review of the Environmental Protection Agency's draft IRIS assessment of tetrachloroethylene. National Academies Press, Washington D.C.

NTP. 1986. National Toxicology Program, U.S. Department of Health and Human Services. Toxicology and carcinogenesis studies of tetrachloroethylene (perchloroethylene) (CAS no. 127-18-4) in F344/N rats and B6C3F1 mice (inhalation studies). Research Triangle Park, NC. NTP Report no. TR 311.

NTP. 2014. National Toxicology Program, U.S. Department of Health and Human Services. National Institutes of Health. 13th Report on Carcinogens. October 2, 2014.

Odum J, Green T, Foster JR, Hext PM. 1988. The role of trichloroacetic acid and peroxisome proliferation in the differences in carcinogenicity of perchloroethylene in the mouse and rat. *Toxicology and Applied Pharmacology* 92:103-112.

OEHHA. 1992. Office of Environmental Health Hazard Assessment. Health Effects of Perchloroethylene. May 1992.

OEHHA. 2001. Office of Environmental Health Hazard Assessment. Public Health Goal for Tetrachloroethylene in Drinking Water. August 2001.

OEHHA. 2009. Office of Environmental Health Hazard Assessment. Technical Support Document for Cancer Potency Factors. May 2009.

OEHHA. 2012. Office of Environmental Health Hazard Assessment. Technical Support Document for Exposure Assessment and Stochastic Analysis. August 2012.

Ohtsuki T, Sato K, Koizumi A, Kumai M, Ikeda M. 1983. Limited capacity of humans to metabolize tetrachloroethylene. *International Archives of Occupational and Environmental Health* 51:381-90.

Reddy MB. 2005. Physiologically based pharmacokinetic modeling: science and applications. Wiley-Interscience.

Rooseboom M, Vermeulen NP, Groot EJ, Commandeur JN. 2002. Tissue distribution of cytosolic beta-elimination reactions of selenocysteine Se-conjugates in rat and human. *Chemico-Biological Interactions* 140:243-264.

Seiji K, Jin C, Watanabe T, Nakatsuka H, Ikeda M. 1990. Sister chromatid exchanges in peripheral lymphocytes of workers exposed to benzene, trichloroethylene, or tetrachloroethylene, with reference to smoking habits. *International Archives of Occupational and Environmental Health* 62:171-176.

Schreiber JS, Hudnell HK, Geller AM, House DE, Aldous KM, Force MS, Langguth K, Prohonic EJ, Parker JC, 2002. Apartment residents' and day care workers' exposures to tetrachloroethylene and deficits in visual contrast sensitivity. *Environmental Health Perspectives*. 110:655-664.

Sokol L, Loughran TP, Jr. 2006. Large granular lymphocyte leukemia. *Oncologist* 11:263-273.

Thomas J, Haseman JK, Goodman JI, Ward JM, Loughran TP, Jr., Spencer PJ. 2007. A review of large granular lymphocytic leukemia in Fischer 344 rats as an initial step toward evaluating the implication of the endpoint to human cancer risk assessment. *Toxicological Sciences* 99:3-19.

Tiruppathi C, Miyamoto Y, Ganapathy V, Roesel RA, Whitford GM, Leibach FH. 1990. Hydrolysis and transport of proline-containing peptides in renal brush-border membrane vesicles from dipeptidyl peptidase IV-positive and dipeptidyl peptidase IV-negative rat strains. *Journal of Biological Chemistry* 265:1476-83.

Toraason M, Butler MA, Ruder A, Forrester C, Taylor L, Ashley DL, Mathias P, Marlow KL, Cheever KL, Krieg E, Wey H. 2003. Effect of perchloroethylene, smoking, and race on oxidative DNA damage in female dry cleaners. *Mutation Research/Genetic Toxicology and Environmental Mutagenesis* 539:9-18.

- Tucker JD, Sorensen KJ, Ruder AM, McKernan LT, Forrester CL, Butler MA. 2011. Cytogenetic analysis of an exposed-referent study: perchloroethylene-exposed dry cleaners compared to unexposed laundry workers. *Environmental Health* 10:16.
- USEPA. 1991. Alpha-2u-globulin: Association with chemically induced renal toxicity and neoplasia in the male rat. Washington, DC: U.S. Environmental Protection Agency, National Center for Environmental Assessment. Report no. EPA/625/3-91/019F.
- USEPA. 1992. Draft report: A cross-species scaling factor for carcinogen risk assessment based on equivalence of mg/kg(3/4)/day. *Federal Register* 57:24151-24173.
- USEPA. 2005. U.S. Environmental Protection Agency. Guidelines for carcinogen risk assessment. Risk Assessment Forum. Report no. EPA/630/P-03/001F.
- US EPA. 2011. U.S. Environmental Protection Agency. Toxicological Review of Trichloroacetic Acid, In Support of Summary Information on the Integrated Risk Information System (IRIS), Report no. EPA/635/R-09/003F.
- US EPA. 2012a. U.S. Environmental Protection Agency. Toxicological Review of Tetrachloroethylene (Perchloroethylene), In Support of Summary Information on the Integrated Risk Information System (IRIS). Report no. EPA/635/R-08/011F.
- US EPA. 2012b. U.S. Environmental Protection Agency. Integrated Risk Information System (IRIS) Chemical Assessment Summary: Tetrachloroethylene (Perchloroethylene).
- US EPA. 2012c. U.S. Environmental Protection Agency. Lymphohematopoietic Cancers Induced by Chemicals and Other Agents: Overview and Implications for Risk Assessment, EPA/600/R-10/095F.
- US EPA. 2015. U.S. Environmental Protection Agency, National Center for Environmental Assessment. Benchmark Dose Software (BMDS) Version 2.6.0.1.
- Vamvakas S, Dekant W, Berthold K, Schmidt S, Wild D, Henschler D. 1987. Enzymatic transformation of mercapturic acids derived from halogenated alkenes to reactive and mutagenic intermediates. *Biochemical Pharmacology* 36:2741-2748.
- Vamvakas S, Dekant W, Henschler D. 1989a. Genotoxicity of haloalkene and haloalkane glutathione S-conjugates in porcine kidney cells. *Toxicology in Vitro* 3:151-156.
- Vamvakas S, Herkenhoff M, Dekant W and Henschler D. 1989b. Mutagenicity of tetrachloroethene in the Ames test—metabolic activation by conjugation with glutathione. *Journal of Biochemical Toxicology*. 4:21–27.
- Van Duuren BL, Kline SA, Melchionne S, Seidman I. 1983. Chemical structure and carcinogenicity relationships of some chloroalkene oxides and their parent olefins. *Cancer Research*. 43:159-162.
- Vlaanderen J, Straif K, Ruder A, Blair A, Hansen J, Lynge E, Charbotel B, Loomis D, Kauppinen T, Kyronen P, Pukkala E, Weiderpass E, Guha N. 2014. Tetrachloroethylene exposure and bladder cancer risk: a meta-analysis of dry-cleaning-worker studies. *Environmental Health Perspectives*. 122:661-666.

- Volkel W, Friedewald M, Lederer E, Pahler A, Parker J, Dekant W, 1998. Biotransformation of perchloroethene: dose-dependent excretion of trichloroacetic acid, dichloroacetic acid, and N-acetyl-S-(trichlorovinyl)-L-cysteine in rats and humans after inhalation. *Toxicology and Applied Pharmacology*. 153:20-27.
- Walles SA. 1986. Induction of single-strand breaks in DNA of mice by trichloroethylene and tetrachloroethylene. *Toxicology Letters* 31:31-35.
- Wang JL, Chen WL, Tsai SY, Sung PY, Huang RN. 2001. An *in vitro* model for evaluation of vaporous toxicity of trichloroethylene and tetrachloroethylene to CHO-K1 cells. *Chemico-Biological Interactions* 137:139-154.
- Wheeler JB, Stourman NV, Their R, Dommermuth A, Vuilleumier S, Rose JA, Armstrong RN, Guengerich FP, 2001. Conjugation of haloalkanes by bacterial and mammalian glutathione transferases: mono- and dihalomethanes. *Chemical Research in Toxicology* 14:1118-1127.
- White IN, Razvi N, Gibbs AH, Davies AM, Manno M, Zaccaro C, De Matteis F, Pahler A, Dekant W. 2001. Neoantigen formation and clastogenic action of HCFC-123 and perchloroethylene in human MCL-5 cells. *Toxicology Letters* 124:129-138.
- Yang Q, Ito S, Gonzalez FJ. 2007. Hepatocyte-restricted constitutive activation of PPAR alpha induces hepatoproliferation but not hepatocarcinogenesis. *Carcinogenesis* 28:1171-1177.
- Yoo HS, Bradford BU, Kosyk O, Shymonyak S, Uehara T, Collins LB, Bodnar WM, Ball LM, Gold A, Rusyn I. 2015. Comparative analysis of the relationship between trichloroethylene metabolism and tissue-specific toxicity among inbred mouse strains: liver effects. *Journal of Toxicology and Environmental Health A*. 78:15-31.
- Yoshioka T, Krauser JA, Guengerich FP. 2002. Tetrachloroethylene oxide: hydrolytic products and reactions with phosphate and lysine. *Chemical Research in Toxicology* 15:1096-1105.

**APPENDIX A**

**PBPK Model Code for Simplified, Inhalation-Only Adaptation of Chiu and Ginsberg  
(2011) PCE Model, for Mice, Rats, and Humans  
(Written in Berkeley Madonna)**

{ Inhalation-Only Adaptation of Chiu and Ginsberg (2010) PCE Model  
for MICE }

```
METHOD RK4
STARTTIME = 0
STOPTIME=504
DT = 0.002

ppm=10      {inhaled conc in ppm}
CInh=If (Mod(Time,24)<=6 AND Mod(Time,168)<=120) Then (ppm*165.83/24450) Else 0

; BW=0.037 {NTP Male}
; BW=0.048 {JISHA Male}
; BW=0.025 {NTP Female}
  BW=0.035 {JISHA Female}

QC=11.6*BW^0.75
QP=QC*2.5*exp(0.325015)
QM=QP/0.7    {minute volume, L/h}
DResp=QP*exp(0.203)
; Intake=QM*Cinh*24/BW

QGut=0.141*QC
QLiv=0.02*QC
QKid=0.091*QC
QFat=0.07*QC
QRap=0.461*QC
QSlw=0.217*QC

PB=18.6
PResp=79.1/PB
PGut=62.1/PB
PLiv=48.8/PB
PKid=79.1/PB
PRap=62.1/PB
PSlw=79.1/PB
PFat=1510.8/PB

VResp=0.0007*BW
VRespEff=VResp*PResp*PB
VRespLum=0.004667*BW
VGut=0.049*BW
VLiv=0.055*BW
VKid=0.017*BW
VRap=0.1*BW
VFat=0.07*BW
VBld=0.049*BW
VSlw=(0.8897*BW)-(VResp+VGut+VLiv+VKid+VRap+VFat+VBld)

{ Metabolic Constant Calculations }
{=====}
KMo=          88.6
lnKMC=       -5.35885
ClCo=        1.57
lnClC=       3.18103
lnKM2C=      15
lnCl2OxC=   -1.20051
KmKidLivo=   0.616
```

Perchloroethylene Inhalation Cancer Potency Values  
SRP REVIEW DRAFT

May, 2016

ClKidLivo= 0.0211  
VMaxLungLivo= 0.07  
VMaxTCVGo= 35.3  
lnVMaxTCVGC= 10.2  
ClTCVGo= 0.656  
lnClTCVGC= -9.17006  
VMaxKidLivTCVGo= 0.15  
ClKidLivTCVGo= 0.24

KM=KMo\*exp(lnKMC)  
VMax= KM\*ClCo\*VLiv\*exp(lnClC)

KM2=KM\*exp(lnKM2C)  
VMax2=KM2\*(VMax/KM)\*exp(lnCl2OxC)

KMKid=KM\*KMKidLivo  
VMaxKid=(VMax/KM)\*KMKid\*(VKid/VLiv)\*ClKidLivo

KMClara=KM\*PLiv/(PB\*PResp)  
VMaxClara=VMax\*VMaxLungLivo

VMaxTCVG=VMaxTCVGo\*VLiv\*exp(lnVMaxTCVGC)  
KmTCVG=VMaxTCVG/(ClTCVGo\*exp(lnClTCVGC))

VMaxKidTCVG=VMaxTCVG\*(VKid/VLiv)\*VMaxKidLivTCVGo  
KmKidTCVG=VMaxKidTCVG/(ClKidLivTCVGo\*(VKid/VLiv)\*(VMaxTCVG/KmTCVG))  
{=====}

Init AGut=0 Limit AGut>=0  
Init AResp=0 Limit AResp>=0  
Init AExhResp=0 Limit AExhResp>=0  
Init AInhResp=0 Limit AInhResp>=0  
Init ALiv=0 Limit ALiv>=0  
Init AKid=0 Limit AKid>=0  
Init ARap=0 Limit ARap>=0  
Init ASlw=0 Limit ASlw>=0  
Init AFat=0 Limit AFat>=0  
Init ABld=0 Limit ABld>=0

{Respiratory Model Concentrations}

CInhResp=AInhResp/VRespLum {conc resp lumen during inh, mg/L}  
CResp=AResp/VRespEff {conc resp tract tissue, mg/L}  
CExhResp=AExhResp/VRespLum {conc resp lumen during exh, mg/L}

{Blood Concentrations}

CVGut=(AGut/VGut)\*(1/PGut)  
CVLiv=(ALiv/VLiv)\*(1/PLiv)  
CVKid=(AKid/VKid)\*(1/PKid)  
CVRap=(ARap/VRap)\*(1/PRap)  
CVSlw=(ASlw/VSlw)\*(1/PSlw)  
CVFat=(AFat/VFat)\*(1/PFat)  
CVBld=(ABld/VBld)  
CArt=(QC\*CVBld+QP\*CInhResp)/(QC+(QP/PB))

{Metabolism: P450 Oxidation}

RAMetLng=(VMaxClara\*CResp)/(KMClara+CResp)  
RAMetLiv1=(VMax\*CVLiv)/(KM+CVLiv)+(VMax2/KM2)\*CVLiv  
RAMetKid1=(VMaxKid\*CVKid)/(KMKid+CVKid)

```
{Metabolism: GST Conjugation}
RAMetLiv2=(VMaxTCVG*CVLiv)/(KMTCVG+CVLiv)
RAMetKid2=(VMaxKidTCVG*CVKid)/(KMKidTCVG+CVKid)

{Respiratory Model Mass Balance Equations}
AInhResp'=QM*CIInh+DResp*(CResp-CInhResp)-QM*CIInhResp
AResp'=DResp*(CInhResp+CEXHResp-2*CResp)-RAMetLNg
AExhResp'=QM*(CInhResp-CEXHResp)+QP*((CArt/PB)-CInhResp)+DResp*(CResp-CEXHResp)

{Other Mass Balance Equations}
AGut'=QGut*(CArt-CVGut)
ALiv'=(QLiv*CArt)+(QGut*CVgut)-((QLiv+QGut)*CVLiv)-RAMetLiv1-RAMetLiv2
AKid'=QKid*(CArt-CVKid)-RAMetKid1-RAMetKid2
ARap'=Qrap*(CArt-CVRap)
ASlw'=QSlw*(CArt-CVSlw)
AFat'=QFat*(CArt-CVfat)
ABld'=(QFat*CVfat)+((QGut+QLiv)*CVLiv)+(QSlw*CVSlw)+(Qrap*CVRap)+(QKid*CVKid)-
(QC*CVBld)

init MetCum=0          Limit MetCum>=0
init LivOxCum=0       Limit LivOxCum>=0

MetTot=RAMetLNg+RAMetLiv1+RAMetKid1+RAMetLiv2+RAMetKid2
MetCum'=If TIME>=336 Then (MetTot/(7*BW)) Else 0
LivOxCum'=If TIME>=336 Then (RAMetLiv1/(7*BW)) Else 0
```

{ Inhalation-Only Adaptation of Chiu and Ginsberg (2011) PCE Model  
for RATS }

```
METHOD RK4
STARTTIME = 0
STOPTIME=504
DT = 0.002

ppm=50      {inhaled conc in ppm}
CInh=If (Mod(Time,24)<=6 AND Mod(Time,168)<=120) Then (ppm*165.83/24450) Else 0

; BW=0.44   {NTP Male}
  BW=0.45   {JISHA Male}
; BW=0.32   {NTP Female}
; BW=0.30   {JISHA Female}

QC=13.3*BW^0.75
QP=QC*1.9*0.61643
QM=QP/0.7   {minute volume, L/h}
DResp=QP*exp(1)
; Intake=QM*Cinh*24/BW

QGut=0.153*QC
QLiv=0.021*QC
QKid=0.141*QC
QFat=0.07*QC
QRap=0.279*QC
QSlw=0.336*QC

PB=15.1
PResp=32.7/PB
PGut=40.6/PB
PLiv=50.3/PB
PKid=32.7/PB
PRap=40.4/PB
PSlw=21.6/PB
PFat=1489.3/PB

VResp=0.0005*BW
VRespEff=VResp*PResp*PB
VRespLum=0.004667*BW
VGut=0.032*BW
VLiv=0.034*BW
VKid=0.007*BW
VRap=0.088*BW
VFat=0.07*BW
VBld=0.074*BW
VSlw=(0.8995*BW)-(VResp+VGut+VLiv+VKid+VRap+VFat+VBld)

{ Metabolic Constant Calculations }
{=====}
KMo=          69.7
lnKMC=        -0.805889
ClCo=         0.36
lnClC=        2.02965
KMKidLivo=    1.53
ClKidLivo=    0.0085
VMaxLungLivo= 0.0144
```

Perchloroethylene Inhalation Cancer Potency Values  
SRP REVIEW DRAFT

May, 2016

VmaxTCVGo= 93.9  
lnVMaxTCVGC= 10.2  
ClTCVGo= 2.218  
lnClTCVGC= -6.99311  
VMaxKidLivTCVGo= 0.15  
ClKidLivTCVGo= 0.098

KM=KMo\*exp(lnKMC)  
VMax=KM\*ClCo\*VLiv\*exp(lnClC)

KMKid=KM\*KMKidLivo  
VMaxKid=(VMax/KM)\*KMKid\*(VKid/VLiv)\*ClKidLivo

KMClara=KM\*PLiv/(PB\*PResp)  
VMaxClara=VMax\*VMaxLungLivo

VMaxTCVG=VMaxTCVGo\*VLiv\*exp(lnVMaxTCVGC)  
KmTCVG=VMaxTCVG/(ClTCVGo\*exp(lnClTCVGC))

VMaxKidTCVG=VMaxTCVG\*(VKid/VLiv)\*VMaxKidLivTCVGo  
KmKidTCVG=VMaxKidTCVG/(ClKidLivTCVGo\*(VKid/VLiv)\*(VMaxTCVG/KMTCVG))  
{=====}

Init AGut=0                   Limit AGut>=0  
Init AResp=0                  Limit AResp>=0  
Init AExhResp=0               Limit AExhResp>=0  
Init AInhResp=0               Limit AInhResp>=0  
Init ALiv=0                   Limit ALiv>=0  
Init AKid=0                   Limit AKid>=0  
Init ARap=0                   Limit ARap>=0  
Init ASlw=0                   Limit ASlw>=0  
Init AFat=0                   Limit AFat>=0  
Init ABld=0                   Limit ABld>=0

{Respiratory Model Concentrations}  
CInhResp=AInhResp/VRespLum    {conc resp lumen during inh, mg/L}  
CResp=AResp/VRespEff           {conc resp tract tissue, mg/L}  
CExhResp=AExhResp/VRespLum    {conc resp lumen during exh, mg/L}

{Blood Concentrations}  
CVGut=(AGut/VGut)\*(1/PGut)  
CVLiv=(ALiv/VLiv)\*(1/PLiv)  
CVKid=(AKid/VKid)\*(1/PKid)  
CVRap=(ARap/VRap)\*(1/PRap)  
CVSlw=(ASlw/VSlw)\*(1/PSlw)  
CVFat=(AFat/VFat)\*(1/PFat)  
CVBld=(ABld/VBld)  
CArt=(QC\*CVBld+QP\*CInhResp)/(QC+(QP/PB))

{Metabolism: P450 Oxidation}  
RAMetLiv1=(VMax\*CVLiv)/(KM+CVLiv)  
RAMetKid1=(VMaxKid\*CVKid)/(KMKid+CVKid)  
RAMetLng=(VMaxClara\*CResp)/(KMClara+CResp)

{Metabolism: GST Conjugation}  
RAMetLiv2=(VMaxTCVG\*CVLiv)/(KMTCVG+CVLiv)  
RAMetKid2=(VMaxKidTCVG\*CVKid)/(KMKidTCVG+CVKid)

```
{Respiratory Model Mass Balance Equations}
AInhResp'=QM*CIInh+DResp*(CResp-CInhResp)-QM*CIInhResp
AResp'=DResp*(CIInhResp+CEXHResp-2*CResp)-RAMetLNg
AExhResp'=QM*(CIInhResp-CEXHResp)+QP*((CART/PB)-CIInhResp)+DResp*(CResp-CEXHResp)
```

```
{Other Mass Balance Equations}
AGut'=QGut*(CART-CVGut)
ALiv'=(QLiv*CART)+(QGut*CVgut)-((QLiv+QGut)*CVLiv)-RAMetLiv1-RAMetLiv2
AKid'=QKid*(CART-CVKid)-RAMetKid1-RAMetKid2
ARap'=Qrap*(CART-CVRap)
ASlw'=QSlw*(CART-CVSlw)
AFat'=QFat*(CART-CVFat)
ABld'=(QFat*CVFat)+((QGut+QLiv)*CVLiv)+(QSlw*CVSlw)+(Qrap*CVrap)+(QKid*CVKid)-
(QC*CVBld)
```

```
init MetCum=0      Limit MetCum>=0
```

```
MetTot=RAMetLNg+RAMetLiv1+RAMetKid1+RAMetLiv2+RAMetKid2
MetCum'=If TIME>=336 Then (MetTot/(7*BW)) Else 0
```

{ Inhalation-Only Adaptation of Chiu and Ginsberg (2011) PCE Model  
for HUMANS }

METHOD RK4  
STARTTIME=0  
STOPTIME=840  
DT = 0.0002

ppm=10 {inhaled conc in ppm}  
CInh=ppm\*165.83/24450

BW=70  
QC=16\*BW^0.75  
QP=0.96\*1.28\*QC  
QM=QP/0.7 {minute volume, L/h}  
DResp=QP\*exp(-5.06)  
; Intake=QM\*Cinh

QGut=0.19\*QC  
QLiv=0.065\*QC  
QKid=0.19\*QC  
QFat=0.05\*QC  
QRap=0.285\*QC  
QSlw=0.22\*QC

PB=14.7  
PResp=58.6/PB  
PGut=59.9/PB  
PLiv=61.1/PB  
PKid=58.6/PB  
PRap=59.9/PB  
PSlw=70.5/PB  
PFat=1450/PB

VResp=0.00018\*BW  
VRespEff=VResp\*PResp\*PB  
VRespLum=0.002386\*BW  
VGut=0.02\*BW  
VLiv=0.025\*BW  
VKid=0.0043\*BW  
VRap=0.088\*BW  
VFat=0.199\*BW  
VBld=0.077\*BW  
VSlw=(0.8560\*BW)-(VResp+VGut+VLiv+VKid+VRap+VFat+VBld)

{ Metabolic Constant Calculations }  
{=====}

KMo=	55.8
lnKMC=	6.9
ClCo=	0.202
lnClC=	0.2501
KMKidLivo=	1.04
ClKidLivo=	0.0125
lnClKidLivC=	4.57452
VMaxLungLivo=	0.0128
VMaxTCVGo=	0.665
lnVMaxTCVGC=	10.2
ClTCVGo=	0.0196

Perchloroethylene Inhalation Cancer Potency Values  
**SRP REVIEW DRAFT**

May, 2016

lnClTCVGC= 5.59162  
 VMaxKidLivTCVGo= 0.15  
 ClKidLivTCVGo= 0.14

KM=KMo\*exp(lnKMC)  
 VMax=KM\*ClCo\*VLiv\*exp(lnClC)

KMKid=KM\*KMKidLivo  
 VMaxKid=(VMax/KM)\*KMKid\*(VKid/VLiv)\*ClKidLivo\*exp(lnClKidLivC)

KMClara=KM\*PLiv/(PB\*PResp)  
 VMaxClara=VMax\*VMaxLungLivo

VMaxTCVG=VMaxTCVGo\*VLiv\*exp(lnVMaxTCVGC)  
 KmTCVG=VMaxTCVG/(ClTCVGo\*exp(lnClTCVGC))

VMaxKidTCVG=VMaxTCVG\*(VKid/VLiv)\*VMaxKidLivTCVGo  
 KmKidTCVG=VMaxKidTCVG/(ClKidLivTCVGo\*(VKid/VLiv)\*(VMaxTCVG/KMTCVG))  
 {=====}

{Metabolism: P450 Oxidation}  
 RAMetLiv1=(Vmax\*CVLiv)/(KM+CVLiv)  
 RAMetKid1=(VMaxKid\*CVKid)/(KMKid+CVKid)  
 RAMetLng=(VMaxClara\*CResp)/(KMClara+CResp)

{Metabolism: GST Conjugation}  
 RAMetLiv2=(VMaxTCVG\*CVLiv)/(KMTCVG+CVLiv)  
 RAMetKid2=(VMaxKidTCVG\*CVKid)/(KMKidTCVG+CVKid)

Init AGut=0                    Limit AGut>=0  
 Init AResp=0                 Limit AResp>=0  
 Init AExhResp=0             Limit AExhResp>=0  
 Init AInhResp=0             Limit AInhResp>=0  
 Init ALiv=0                  Limit ALiv>=0  
 Init AKid=0                  Limit AKid>=0  
 Init ARap=0                  Limit ARap>=0  
 Init ASlw=0                  Limit ASlw>=0  
 Init AFat=0                  Limit AFat>=0  
 Init ABld=0                  Limit ABld>=0

{Respiratory Model Concentrations}  
 CInhResp=AInhResp/VRespLum    {conc resp lumen during inh, mg/L}  
 CResp=AResp/VRespEff         {conc resp tract tissue, mg/L}  
 CExhResp=AExhResp/VRespLum    {conc resp lumen during exh, mg/L}

{Blood Concentrations}  
 CVGut=(AGut/VGut)\*(1/PGut)  
 CVLiv=(ALiv/VLiv)\*(1/PLiv)  
 CVKid=(AKid/VKid)\*(1/PKid)  
 CVRap=(ARap/VRap)\*(1/PRap)  
 CVSlw=(ASlw/VSlw)\*(1/PSlw)  
 CVFat=(AFat/VFat)\*(1/PFat)  
 CVBld=(ABld/VBld)  
 CArt=(QC\*CVBld+QP\*CInhResp)/(QC+(QP/PB))    {arterial blood conc}

{Respiratory Model Mass Balance Equations}  
 AInhResp'=QM\*CInh+DResp\*(CResp-CInhResp)-QM\*CInhResp  
 AResp'=DResp\*(CInhResp+CExhResp-2\*CResp)-RAMetLng  
 AExhResp'=QM\*(CInhResp-CExhResp)+QP\*((CArt/PB)-

$$C_{InhResp} + D_{Resp} * (C_{Resp} - C_{ExhResp})$$

{Other Mass Balance Equations}

$$A_{Gut} = Q_{Gut} * (C_{Art} - C_{VGut})$$

$$A_{Liv} = (Q_{Liv} * C_{Art}) + (Q_{Gut} * C_{Vgut}) - ((Q_{Liv} + Q_{Gut}) * C_{VLiv}) - RAMetLiv1 - RAMetLiv2$$

$$A_{Kid} = Q_{Kid} * (C_{Art} - C_{VKid}) - RAMetKid1 - RAMetKid2$$

$$A_{Rap} = Q_{rap} * (C_{Art} - C_{VRap})$$

$$A_{Slw} = Q_{Slw} * (C_{Art} - C_{VSlw})$$

$$A_{Fat} = Q_{Fat} * (C_{Art} - C_{VFat})$$

$$A_{Bld} = (Q_{Fat} * C_{VFat}) + ((Q_{Gut} + Q_{Liv}) * C_{VLiv}) + (Q_{Slw} * C_{VSlw}) + (Q_{Rap} * C_{VRap}) + (Q_{Kid} * C_{VKid}) - (Q_C * C_{VBld})$$

$$MetTot = (RAMetLng + RAMetLiv1 + RAMetKid1 + RAMetLiv2 + RAMetKid2) * (24 / BW)$$

**APPENDIX B**

**Dose Metric Values used in Dose-Response Modeling  
Obtained from PBPK Inhalation Model**

**PBPK Estimated Total Metabolized Doses**  
(mg/kg-day)

<b>JISHA Mouse</b> (Male and female weights: 0.048 and 0.035 kg)		
<b>Exposure Concentration (ppm)</b>	<b>Male</b>	<b>Female</b>
10	5.10	5.22
50	18.15	18.44
250	72.73	73.94
<b>JISHA Rat</b> (Male and female weights: 0.45 and 0.30 kg)		
<b>Exposure Concentration (ppm)</b>	<b>Male</b>	<b>Female</b>
50	1.82	1.88
200	6.47	6.67
600	15.32	15.83
<b>NTP Mouse</b> (Male and female weights: 0.037 and 0.025 kg)		
<b>Exposure Concentration (ppm)</b>	<b>Male</b>	<b>Female</b>
100	32.78	33.38
200	60.25	61.40
<b>NTP Rat</b> (Male and female weights: 0.44 and 0.32 kg,		
<b>Exposure Concentration (ppm)</b>	<b>Male</b>	<b>Female</b>
200	6.48	6.63
400	11.38	11.66